







Simulations and experimental activities on electron diagnostics for EuPRAXIA@SPARC_LAB

PhD Seminar Third Year 12-11-2025

Candidate:

F. Demurtas

Supervisor:

E. Chiadroni

A. Giribono



Talk outline



- 1. Motivations and goals of the presented thesis work
- Description of the Polarizable X-Band Transverse Deflection Structure system → working principle and field maps studies
- 3. EuPRAXIA@SPARC_LAB Diagnostics simulations for resolution evaluation:
 - Low-energy, middle-energy and high-energy beamline
 - Energy, emittance and longitudinal distribution characterization
- 4. Experimental 3D and 5D reconstruction with the PolariX TDS at SwissFEL
- 5. Summary and conclusions

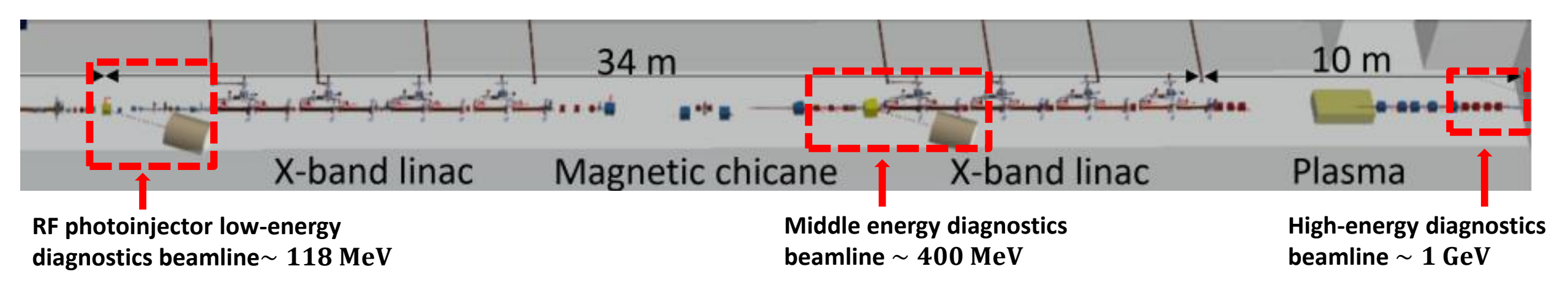


Motivations and goals



Motivations:

The EuPRAXIA@SPARC_LAB project aims to realize the first user-facility based on a Free-Electron Laser driven by a plasma-accelerated beam



Goals of the PhD work

- Implement and characterize the PolariX Transverse Deflection Structure (TDS), focusing on the field maps studies of the 50-cell device
- Evaluate the **resolution limits of the EuPRAXIA diagnostic systems** through beam-dynamics simulations for the three different beamlines
- Application of the 3D and 5D tomographic reconstruction at SwissFEL



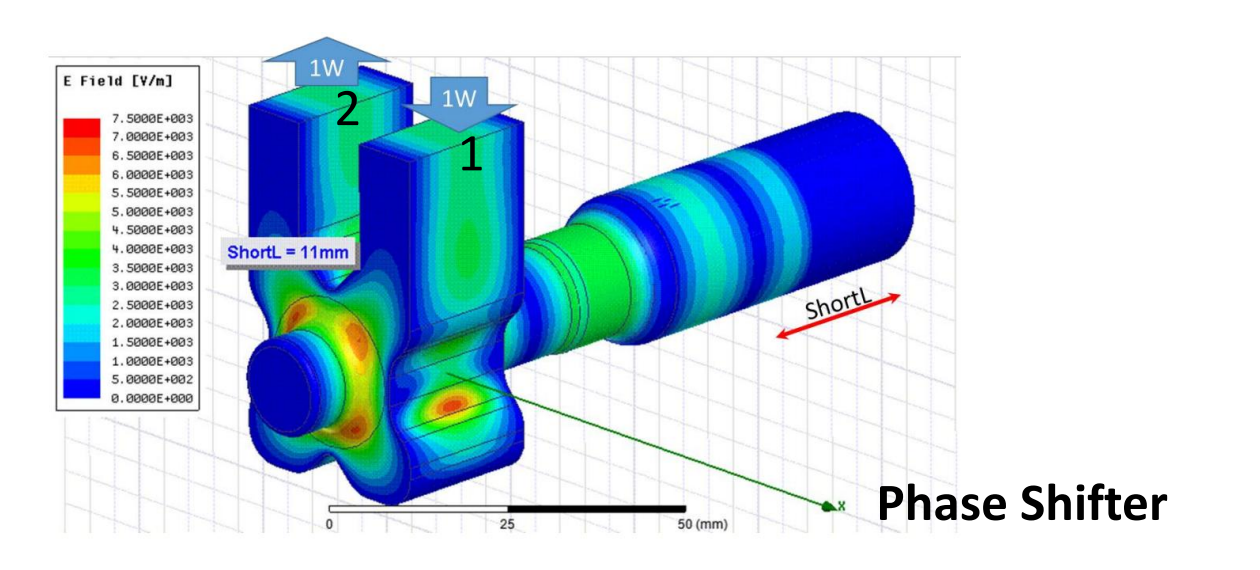
PolariX TDS: RF system

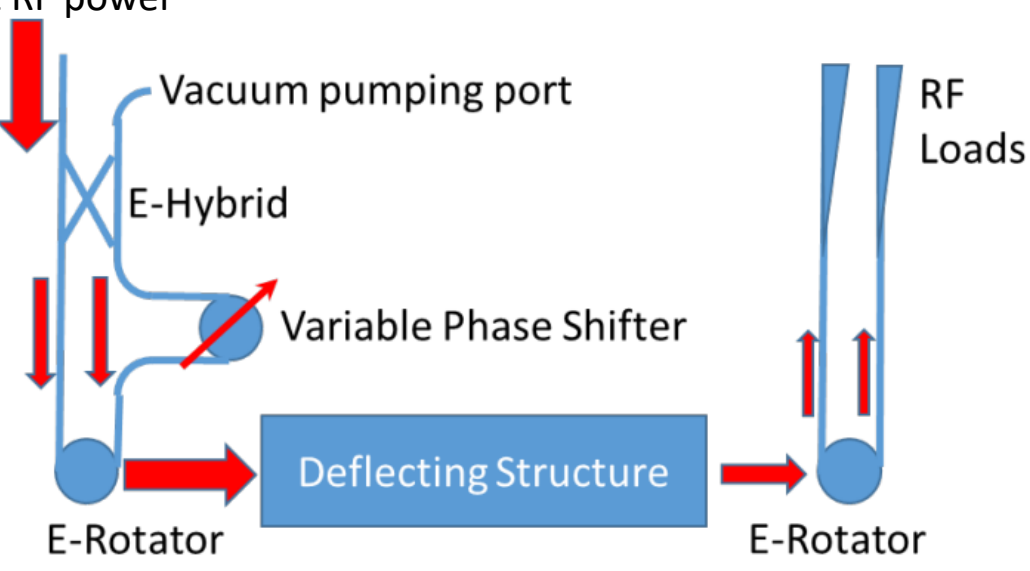


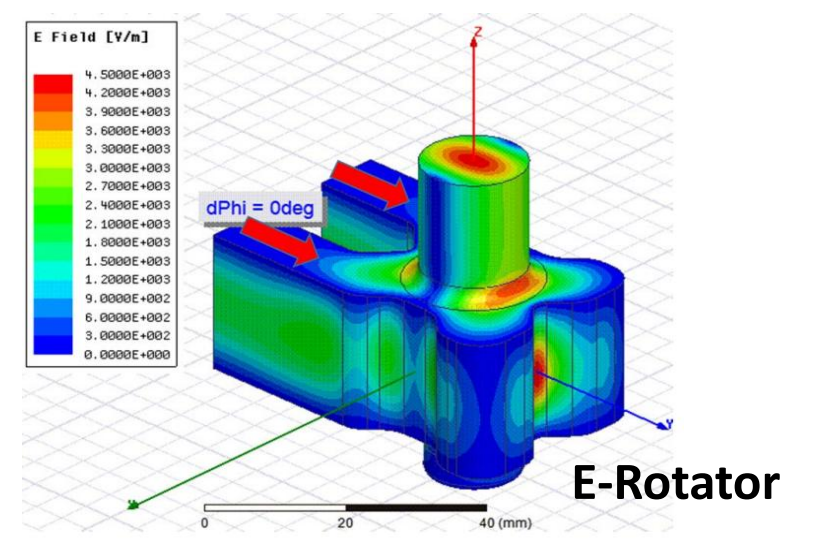
The PolariX is an X-band Transverse Deflection Structure with the feature of changing the beam streaking direction

Input RF power

- The input RF power is split into two branches
- The phase shifter introduces a phase difference between ports 1 and 2:
 - 0 deg -> vertical polarization
 - 180 deg -> horizontal polarization
- The two branches are then recombined into the E-rotator



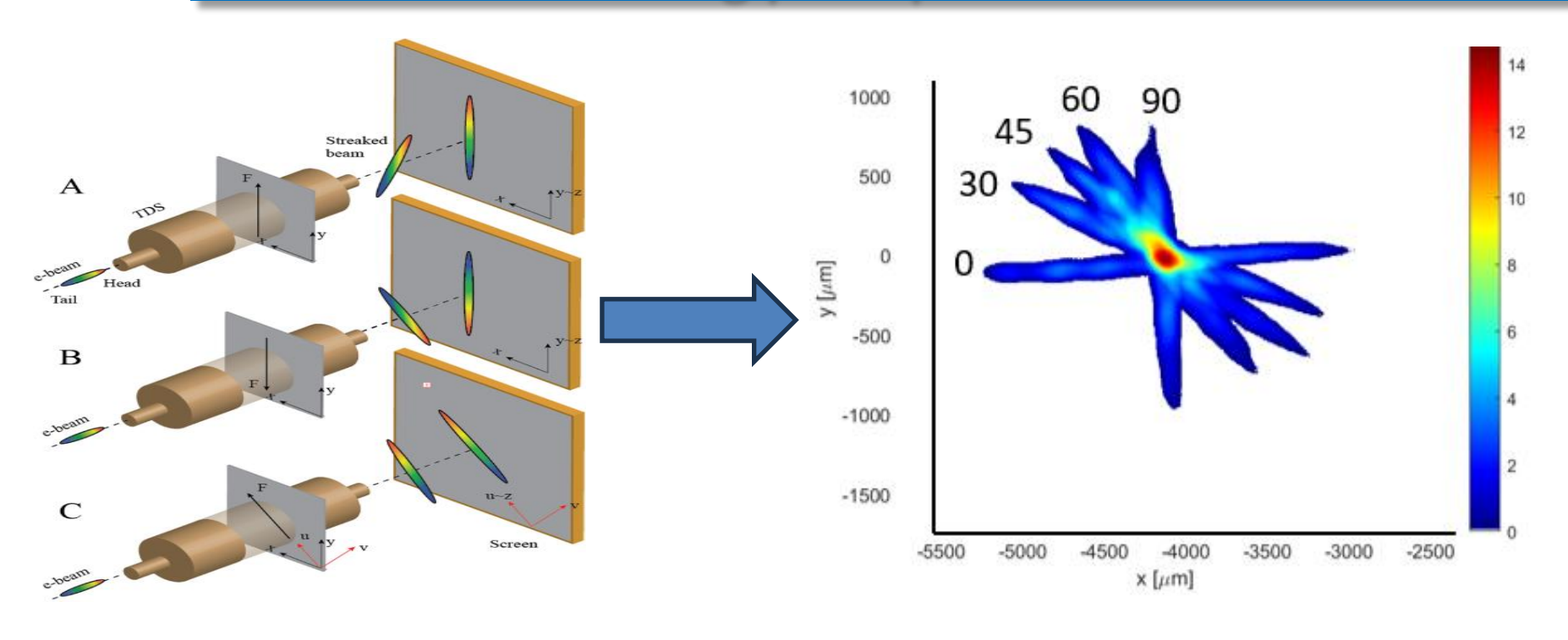






PolariX TDS: Working principle





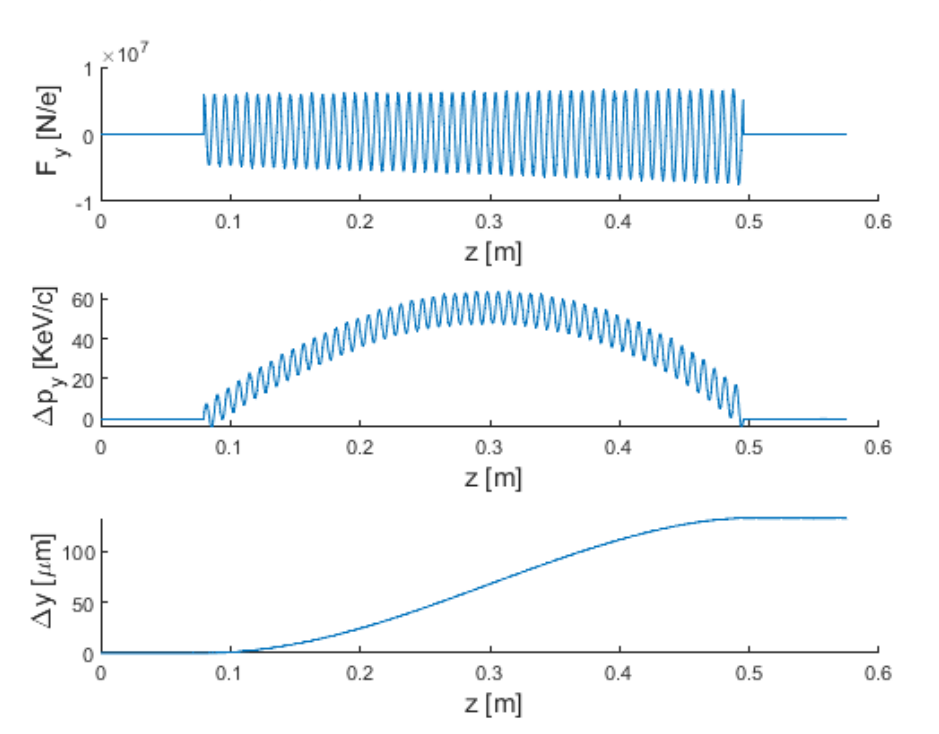
- > It is capable of measuring the longitudinal properties of the beam in both transverse planes with fs-resolution
- Allows for a tomography of the beam to reconstruct the 3D (x,y,t) and 5D (x,x',y,y',t) beam distribution, by streaking the beam for different field polarizations
- > Two PolariX TDS are implemented in the EuPRAXIA diagnostics beamlines:
 - 96-cell structure (~ 1 GeV)
 - 50-cell structure (~ 118 MeV) ⇒ Field maps design

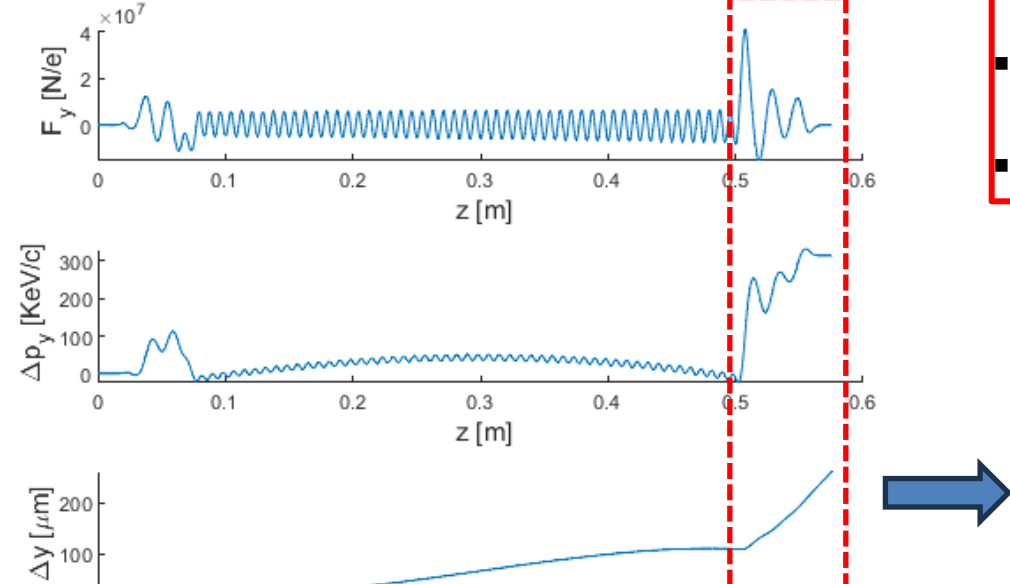


PolariX TDS: Coupler residual kick



Fields maps generated with HFSS to test the effect on the beam dynamics





0.3

z [m]

0.4

0.2

- On-axis field (50-cell)
- 1 W of input power
- Vertical streaking

Residual kick from the output coupler

• Field integral comparison:

Input power: 1 W	96-cells	50-cells
V_{int}	5.24 kV	3.21 kV
V_{int} (no couplers)	5.13 kV	3.05 kV
Difference	~ 2 %	~ 5 %
Power-to-Voltage	$5.2 MV / \sqrt{MW}$	$3.2~MV/\sqrt{MW}$

0.1

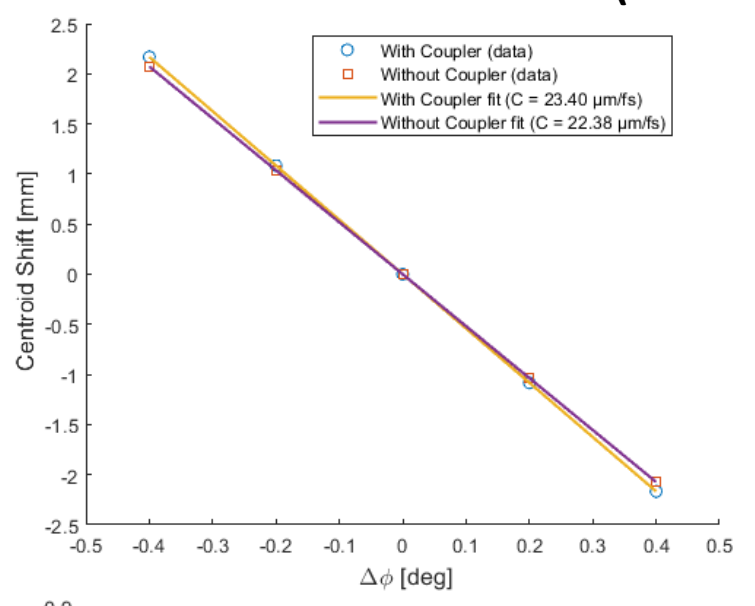
Evaluate the coupler influence on the temporal profile reconstruction



Ideal beam simulations



\succ 50 cells structure simulations (ideal beam at 118 MeV, $\sigma_t=17~fs$)



Parameters	Full structure	No couplers
V[MV]	10.0 ± 0.1	9.6 ± 0.1
$C[\mu m/fs]$	23.4 ± 0.1	22.4 ± 0.1
$R_t[fs]$	~ 4.6	~ 4.9
$\phi_0 [deg]$	~ 74.6	~ 76.2

- Slightly overextimate the longitudinal calibration and resolution
- Slippage effect that changes the zero-crossing phase

	0.9			0.0		Expected TDS On	d
	0.7			Market	_	– – No Coup	bler
	0.6		i d	Walnut A			
স্থ	0.5		, Jr	•	N.		
_	0.4		J		N ₁		
	0.3		1		M		
	0.2	J.	M.		N _A	l.	
	0.1	and the state of			1	M	
	0	- Contraction				The same of the sa	
	-60	-40	-20	0 t [fs]	20	40	60

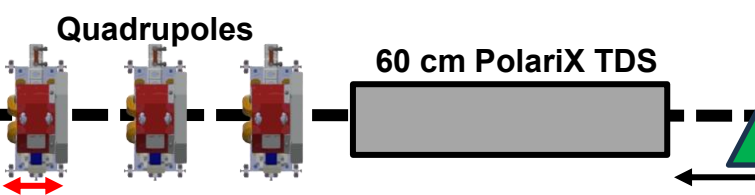
Parameters	Full structure	No couplers
σ_t (sim) [fs]	16.9 ± 0.6	16.8 ± 0.6
σ_t (err) [%]	~ 3.5	~ 3.7
$\sigma_t (diff) [\%]$	~ 0.8	~ 1
σ_e (off) [KeV]	10	0
σ_e (on) [KeV]	~ 275	~ 264

- The reconstruction of the temporal profile is not affected significantly by the coupler contribution
- The induced energy spread does not introduce errors in the measurement



Low-energy beamline: energy measurement





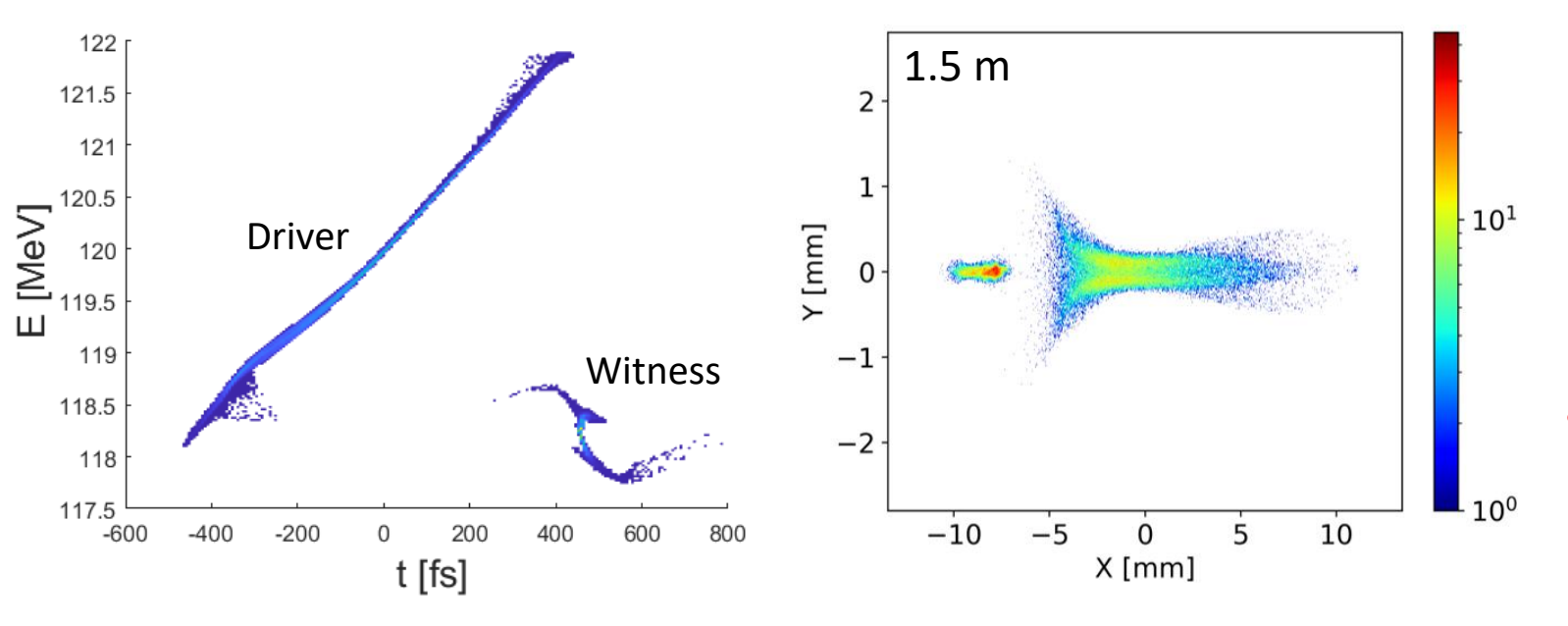




Screen

3.35 m Drift

Energy simulations:



 The screen position provides an optimal trade-off between energy resolution and field of view, allowing to have both driver and witness in the same image

Parameter	Witness	Driver	Unit
E_{mean}	118.2	119.7	MeV
$E_{ m rms}$	156.0	784.8	KeV
FWHM	714.7	3704.3	KeV

Synchrotron-radiation effects are included in the simulation and lead to a slightly broader energy spectrum, without affecting the separation between driver and witness

 The measured energy and relative spread are stable across the explored screen resolutions, confirming the robustness of the diagnostic system

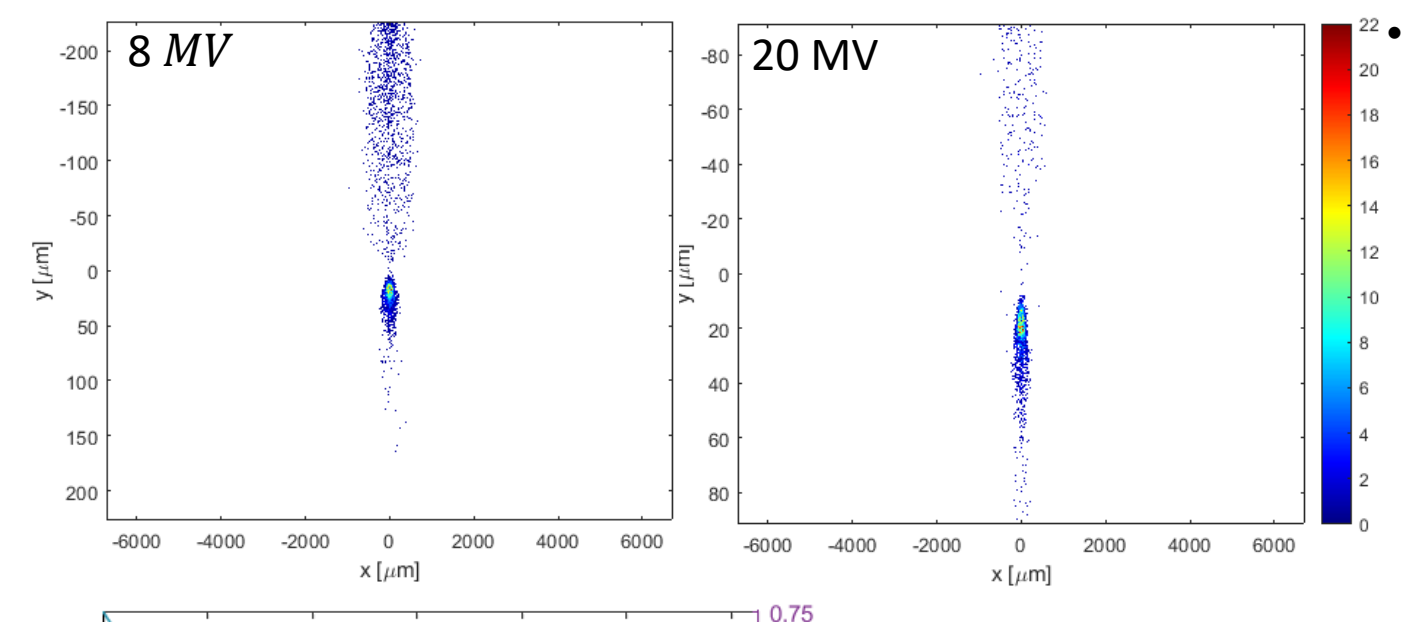
Parameter	3.5 μm	5.25 μm	$7 \mu m$
$(\bar{E}_{dipole} - \bar{E}_{screen})$ [keV]	-34.8	-34.8	-34.8
$(rmsE_{dipole} - rmsE_{screen})$ [keV]	15.4	15.6	15.6
$Min E_{bin} [keV]$	0.66	0.98	1.30
$Max E_{bin} [keV]$	0.67	1.01	1.35
$E_{\rm rms}$ [keV]	156.0	156.3	156.3



Low-energy beamline: TDS measurement

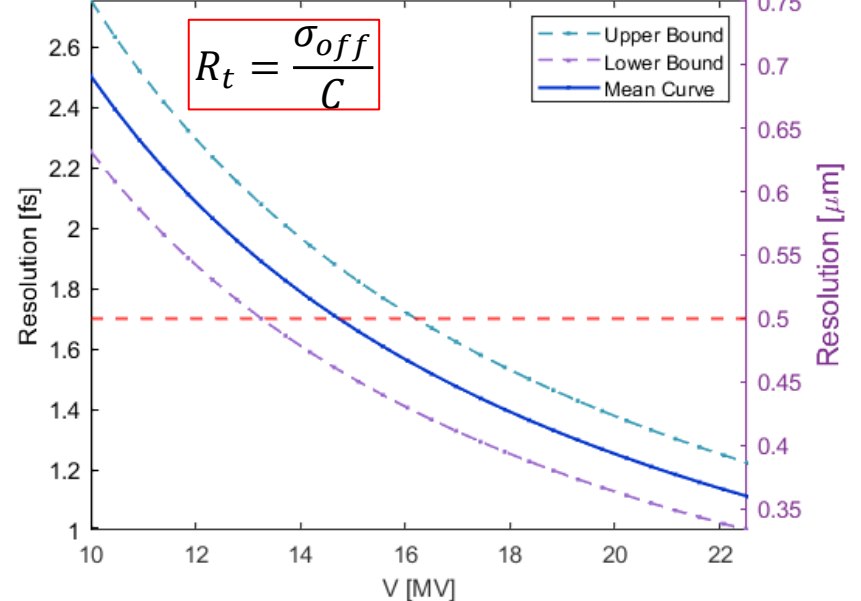


TDS simulations:



The temporal separation between driver and witness increases with the deflecting voltage. For voltages above 8 MV, both bunches are clearly resolved on the screen.

V [MV]	$\mu \mathbf{m}/\mathbf{f}\mathbf{s}$	fs/pixel	Center-Center [fs]	Head-Tail [fs]
1	2.3	3.0	-	-
3	7.0	1.0	509.4	10.4
6	13.9	0.5	507.8	17.0
8	18.5	0.4	507.3	21.5
12	27.8	0.3	504.8	25.3



 The deflector calibration provides a resolution of ≈1 fs at 20 MV

Measured parameters in agreement with the expected input distribution

Parameter	x Streaking	y Streaking
$\sigma_{off} [\mu m]$	54 ± 5	54 ± 5
V [MV]	20.0 ± 0.5	20.0 ± 0.6
Calibration $[\mu m/\text{fs}]$	47 ± 1	47 ± 2
Screen Calibration [fs/pixel]	~ 0.07	~ 0.07
Shear Parameter $[\mu m/\mu m]$	156.2 ± 0.7	156.1 ± 0.7
Resolution [fs]	1.1 ± 0.2	1.1 ± 0.2

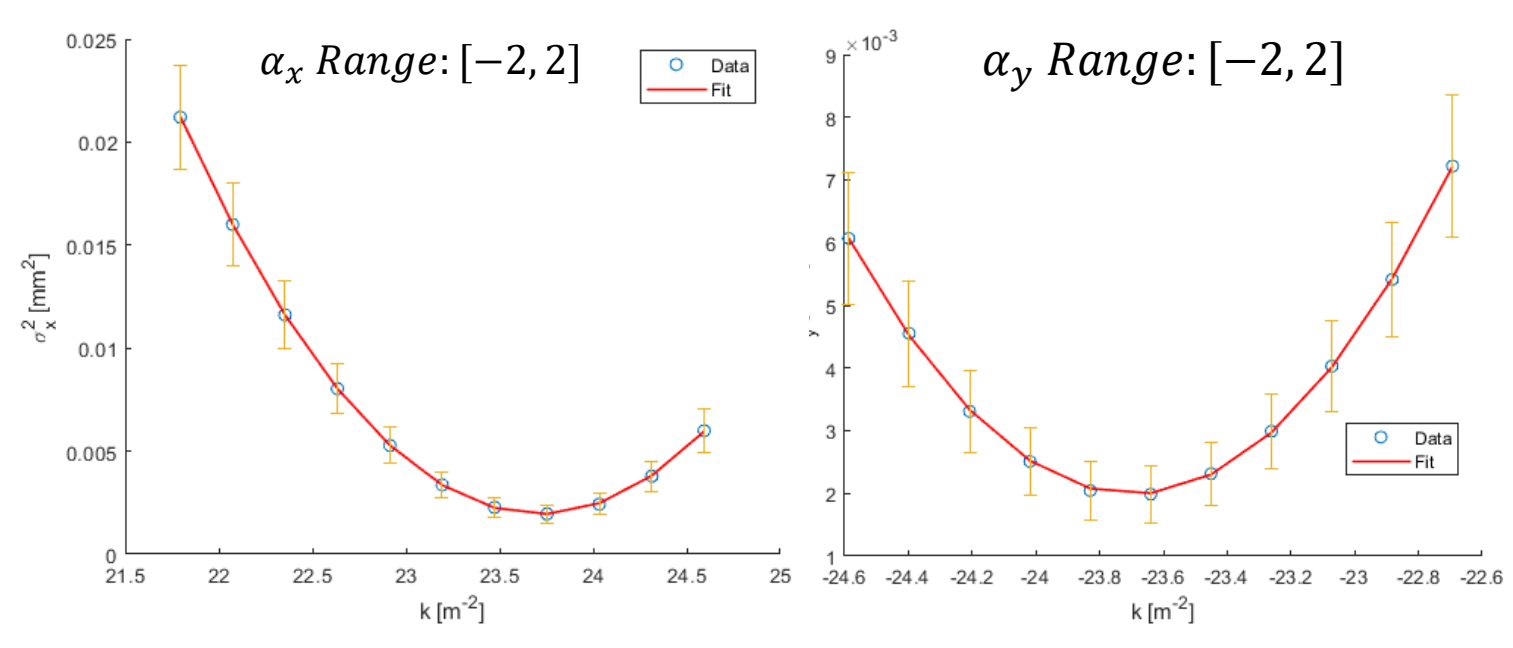
	Witness		Driver	
	x-streaking	y-streaking	x-streaking	y-streaking
σ_t [fs]	16 ± 1	16 ± 1	184 ± 4	192 ± 3
$\bar{\sigma}_t$ [fs]	16 ± 1		188	± 3
σ_t (sim.) [fs]	~ 17		~	191



Low-energy beamline: emittance measurement



Emittance simulations:



 These are the reconstructed values for driver and witness from the simulated scan

Parameters	Witness		Driver	
	\boldsymbol{x}	\boldsymbol{y}	\boldsymbol{x}	\boldsymbol{y}
Input ε_n [mm·mrad]	0.66	0.65	1.50	1.50
Reconstructed ε_n [mm·mrad]	0.68	0.65	1.48	1.46
Error [mm·mrad]	0.05	0.05	0.08	0.06
Relative error [%]	7.7	6.2	5.4	4.1

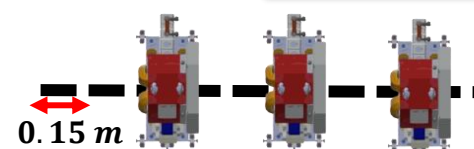
- Accuracy and precision of the reconstructed emittance for decreasing input values.
- The measurement becomes unreliable below $\approx 0.3 \ \mu m$, which is taken as the system's resolution limit.

Plane	Input ε_n	Reconstructed ε_n	Error	Relative error	Difference
	$[mm \cdot mrad]$	$[mm \cdot mrad]$	$[\text{mm}\cdot\text{mrad}]$	[%]	[%]
x	0.50	0.52	0.04	7.6	4.9
x	0.40	0.44	0.03	7.7	9.0
x	0.30	0.34	0.03	8.1	13.1
x	0.20	0.24	0.02	8.6	19.7
x	0.10	0.13	0.01	9.6	33.9
y	0.50	0.52	0.03	4.1	4.9
y	0.40	0.43	0.02	5.1	6.5
y	0.30	0.33	0.02	6.2	9.2
y	0.20	0.23	0.02	7.4	15.2
y	0.10	0.13	0.02	11.8	25.1



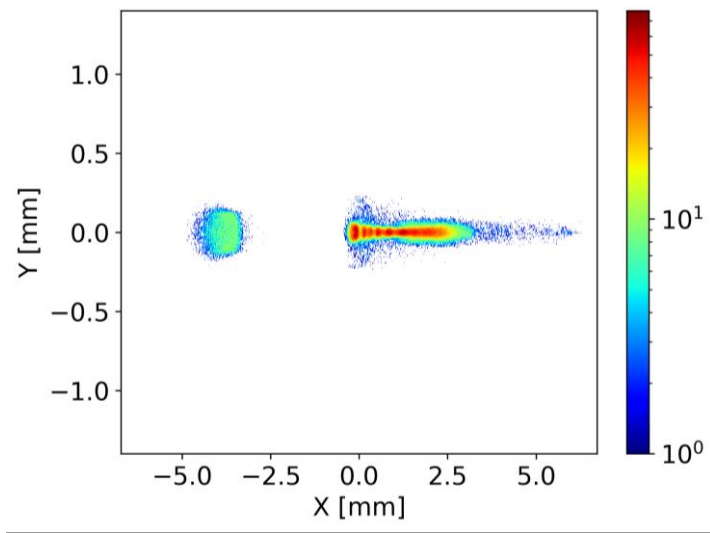
Middle-energy beamline







> Energy simulations:



• At 1.5 m the screen position and resolution allow to clearly measure driver and witness beam in the same image, with sufficient resolution for both bunches

Parameter	Witness	Driver	\mathbf{Unit}
$E_{ m mean}$	402.5	405.9	MeV
$E_{ m rms}$	236.6	762.4	KeV
FWHM	1427.3	2732.1	KeV

Parameter	3.5 μm	5.25 μm	7 μm
$(\bar{E}_{dipole} - \bar{E}_{screen})$ [keV]	-79.9	-79.9	-79.9
$(rmsE_{dipole} - rmsE_{screen})$ [keV]	-9.2	-9.2	-9.2
$Min E_{bin} [keV]$	2.13	3.18	4.22
$\operatorname{Max} E_{bin} [\text{keV}]$	2.18	3.28	4.40
$E_{\rm rms}$ [keV]	236.6	236.6	236.6

Emittance simulations:

Parameters	Wit	ness	Dri	ver
	\boldsymbol{x}	y	\boldsymbol{x}	\boldsymbol{y}
Input ε_n [mm·mrad]	1.40	0.68	1.65	0.74
Reconstructed ε_n [mm·mrad]	1.42	0.64	1.65	0.74
Error [mm·mrad]	0.1	0.08	0.1	0.09
Relative error [%]	7.7	12.1	8.0	11.8

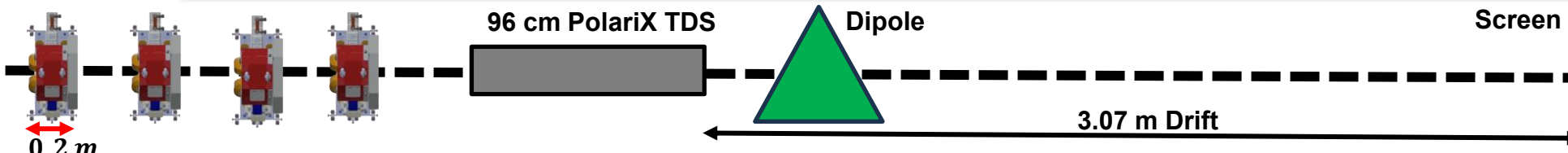
• The measurement becomes unreliable below ≈ 0.2 μm , which is taken as the system's resolution limit

Plane	Input ε_n	Reconstructed ε_n	Error	Rel. error	Difference
	$[\text{mm} \cdot \text{mrad}]$	$[\text{mm} \cdot \text{mrad}]$	$[\text{mm} \cdot \text{mrad}]$	[%]	[%]
x	0.50	0.49	0.03	5.7	2.6
\boldsymbol{x}	0.40	0.39	0.02	6.2	3.0
x	0.30	0.29	0.02	6.7	3.0
x	0.20	0.19	0.01	7.4	3.3
x	0.10	0.10	0.01	8.8	3.5
\overline{y}	0.50	0.54	0.04	6.6	8.9
y	0.40	0.44	0.03	6.9	8.9
y	0.30	0.33	0.02	7.6	8.8
y	0.20	0.22	0.02	8.3	8.7
y	0.10	0.11	0.01	9.8	8.0



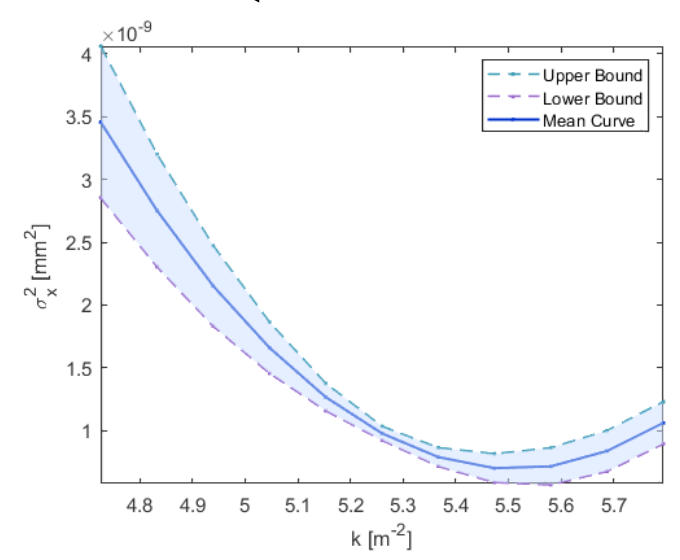
High-energy beamline: emittance

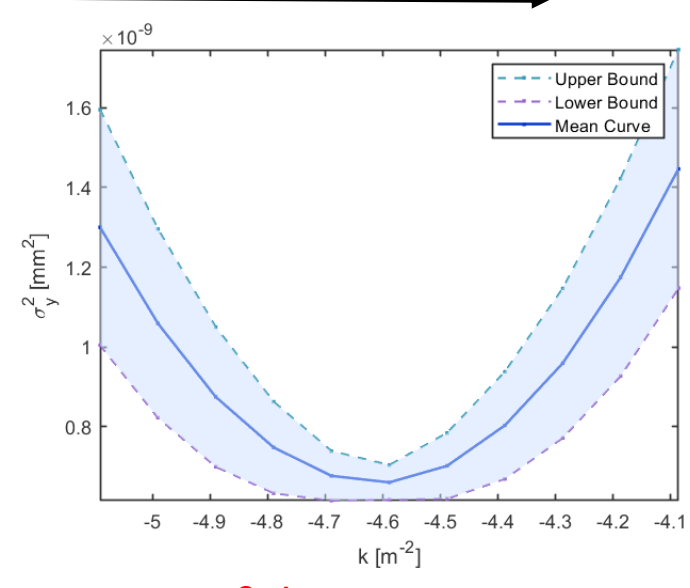




Emittance simulations:

- Quadrupole-scan reconstruction at high energy to take into account shot-to-shot fluctuations in the fitted emittance
- Resolution is not only determined by the instrumental component but also by the shot-to-shot variations





• Considering the shot-to-shot fluctuations the effective emittance resolution at high-energy is $\approx 0.4~\mu m$

Plane	Input ε_n [μm]	Reconstructed $[\mu m]$	Error $[\mu m]$	Rel. error [%]	Diff [%]
x	0.60	0.57	0.05	8.5	5.0
x	0.50	0.47	0.05	9.4	5.6
x	0.40	0.38	0.04	10.7	6.1
x	0.30	0.28	0.03	12.7	7.3
x	0.20	0.18	0.03	16.8	10.8
\overline{y}	0.60	0.64	0.04	6.0	6.8
y	0.50	0.53	0.04	7.1	6.8
y	0.40	0.43	0.04	9.4	6.9
y	0.30	0.32	0.04	12.8	7.2
y	0.20	0.21	0.04	18.1	6.9

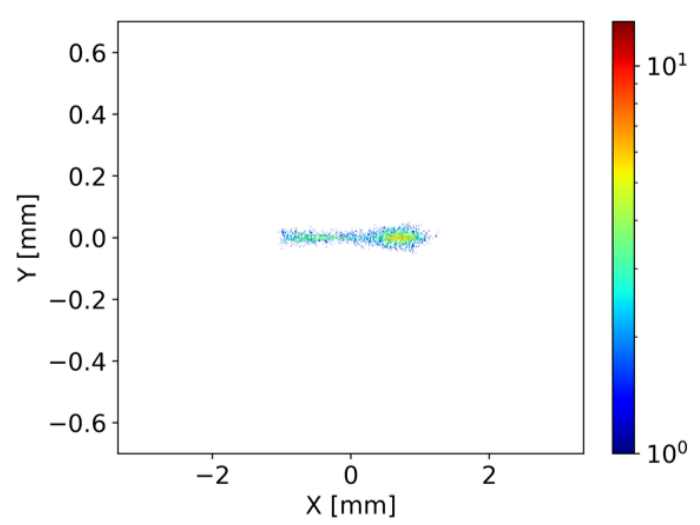
Parameter	Value	
	\mathbf{x}	\mathbf{y}
Input $[\mu m]$	0.85	0.65
Measured $[\mu m]$	0.87	0.63
Standard Deviation $[\mu m]$	0.27	0.26
Instrumental Resolution $[\mu m]$	0	.3
Effective Resolution $[\mu m]$	0	.4



High-energy beamline: LPS Measurement



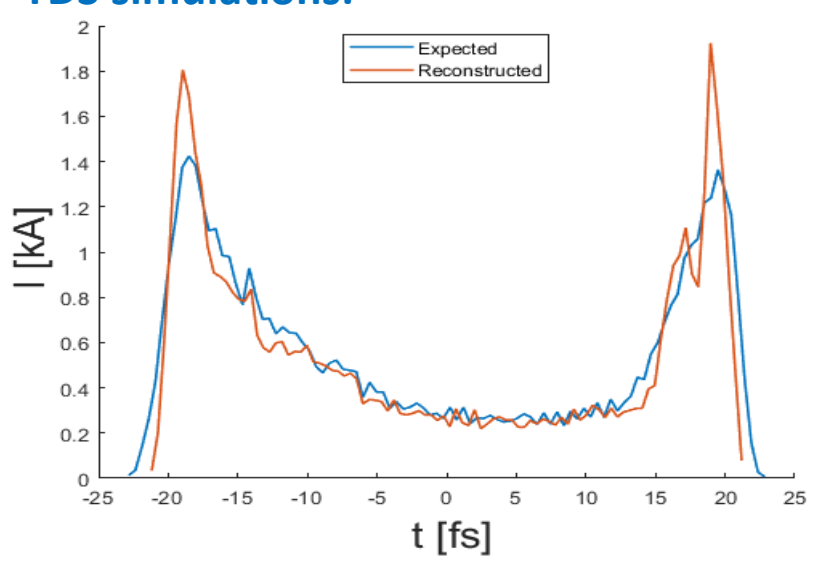
Energy simulations:



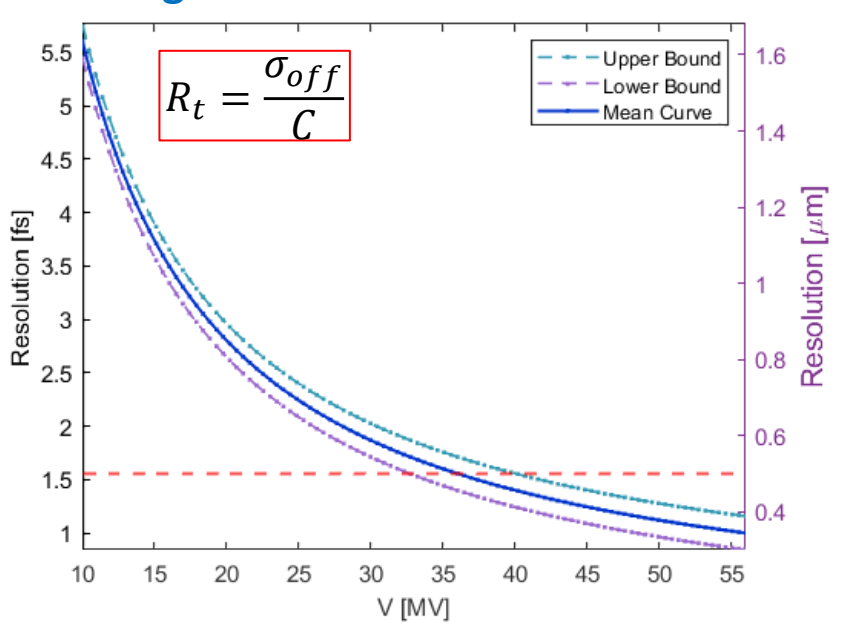
Parameter	Witness	Unit
$E_{ m mean}$	1004.3	MeV
$E_{ m rms}$	932.7	KeV
FWHM	3543.7	KeV

Parameter	$3.5 \mu m$
$(\bar{E}_{dipole} - \bar{E}_{screen})$ [keV]	-63.1
$(rmsE_{dipole} - rmsE_{screen})$ [keV]	-1.5
$Min E_{bin} [keV]$	5.02
$\operatorname{Max} E_{bin} [\text{keV}]$	5.12
$E_{\rm rms}$ [keV]	923.7

> TDS simulations:



Longitudinal resolution:



• The deflector calibration provides a resolution of ≈ 1 fs at 50 MV in vertical streaking and ≈ 2 fs at horizontal streaking, where is limited by the larger unstreaked beam size

Parameter	x Streaking	y Streaking
$\sigma_{off} \ [\mu m]$	28 ± 6	15 ± 5
V [MV]	48.9 ± 0.7	51.4 ± 0.5
Calibration $[\mu m/\mathrm{fs}]$	13.9 ± 0.4	14.6 ± 0.8
Screen Calibration [fs/pixel]	~ 0.25	~ 0.24
Shear Parameter $[\mu m/\mu m]$	46.2 ± 0.3	48.6 ± 0.4
Resolution [fs]	2.0 ± 0.4	1.0 ± 0.2

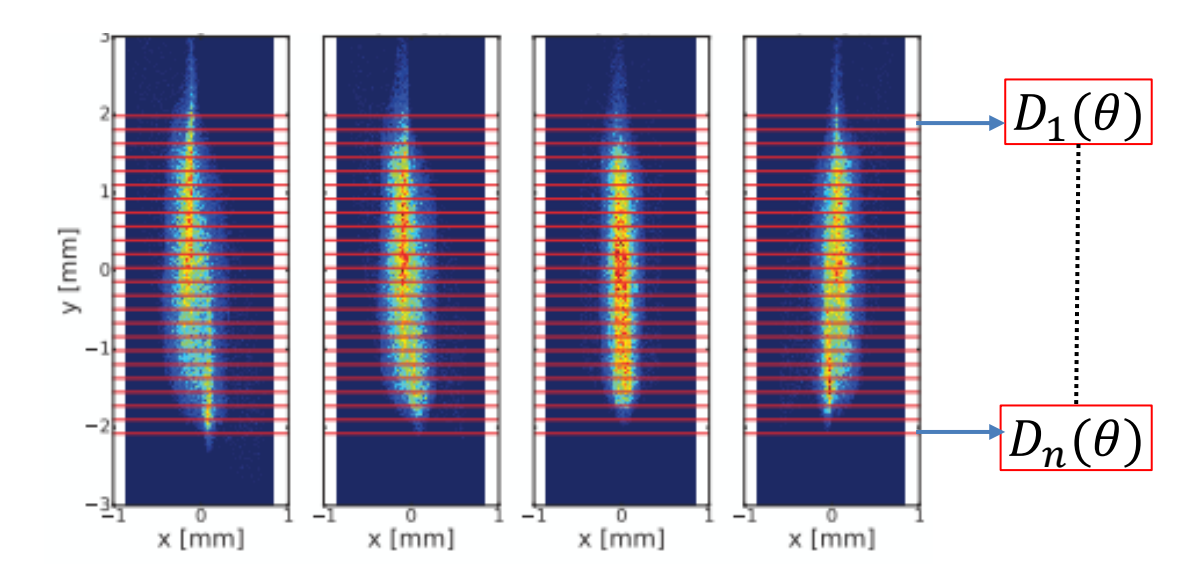
Parameter	x Streaking	y Streaking	
σ_t [fs]	15.0 ± 0.9	14.8 ± 0.9	
$\bar{\sigma_t}$ [fs]	14.9 ± 0.6		
σ_t (sim.) [fs]	~ 14.7		

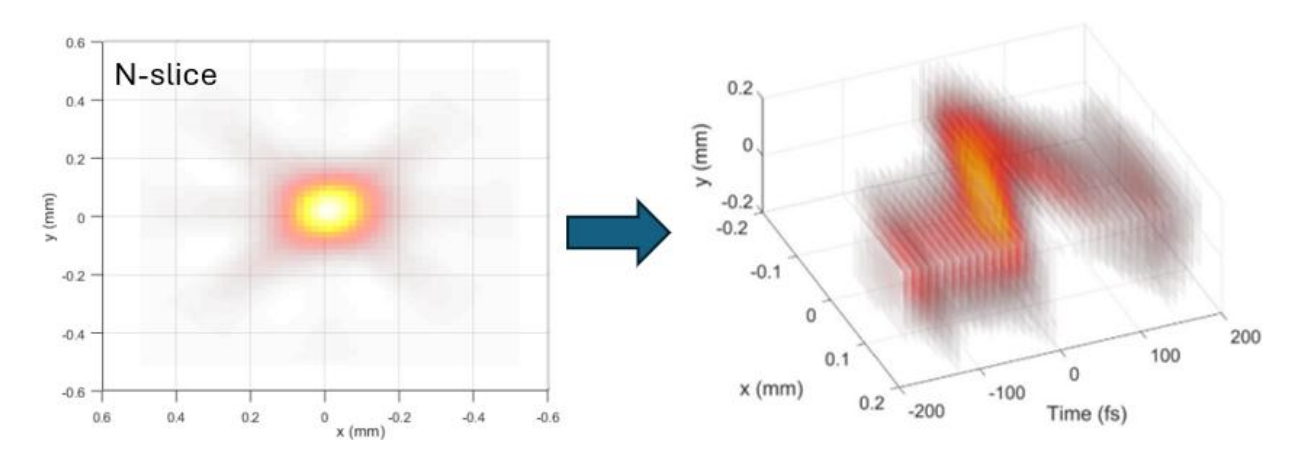


PolariX TDS: Tomographic reconstruction



- The PolariX TDS at high-energy enables the beam characterization through 3D and 5D tomography ⇒ Experimental campaign at the PSI center
 - Combination of two scans:
 - Quadrupole scan → change optics, vary transverse phase advance
 - **PolariX TDS scan** \rightarrow streaking at 10 polarization angles ($\sim 180 \ deg$ coverage)
- ➤ For each quadrupole setting and polarization:
 - Acquire streaked images
 - Each image is divided into longitudinal slices
- 3D Reconstruction
 - Each slice (1D in time) + 10 projections → tomographic 2D reconstruction (x-y)
 - Stacking slices → 3D charge distribution (x, y, t)







PolariX TDS: 5D tomography



> 4D Reconstruction

• 2D slice images interpreted as projections of full 4D phase space (x, x', y, y') rotated by an angle depending on the phase advance

$$I(x,y) = \int \int f_b(x,x',y,y') dx' dy'$$

$$\mu_x \Rightarrow \begin{pmatrix} x_1 \\ x_1' \end{pmatrix} = \begin{pmatrix} \cos(\theta_x) & -\sin(\theta_x) \\ \sin(\theta_x) & \cos(\theta_x) \end{pmatrix} \begin{pmatrix} x \\ x' \end{pmatrix} \Rightarrow I_y(x_1,\theta_x)$$

- $I_{\mathcal{V}}(x_1, \theta_{\mathcal{X}})$ is the projection along the $\theta_{\mathcal{X}}$ direction in the horizontal phase space
- Filtered back-projection algorithm recovers transverse momenta x', y'

$$I_{y,\theta_x}(x)$$
 1° iteration 2° iteration $f(x,x',y,y')$

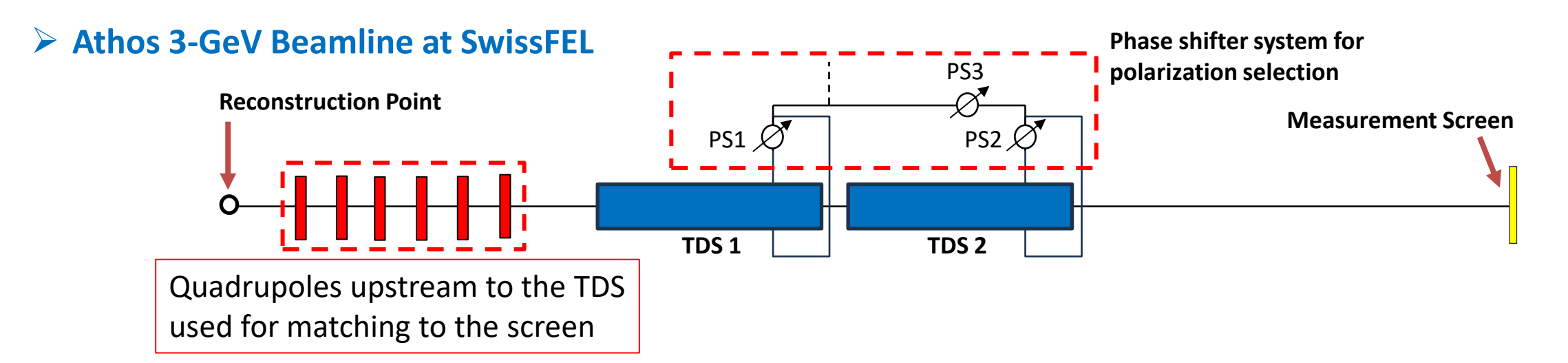
> 5D Reconstruction

- Combine transverse phase space slices (4D) with longitudinal coordinate (t)
- Result: full 5D beam distribution
- Developed and demonstrated for the first time at DESY.



5D Reconstruction: Beamline layout





- Quadrupoles off after the TDS ⇒ Resolution depending on the TDS-screen distance, TDS parameters, and unstreaked beam transverse size at the screen
- System of 3 Phase Shifters needed for polarization selection and opposite kick compensation
- The measurement has been done in two settings: a short bunch $(\sigma_t \sim 19 \ fs)$ and a less compressed $(\sigma_t \sim 40 \ fs)$ to mitigate collective effects in the compressor and reduce the beam tilt

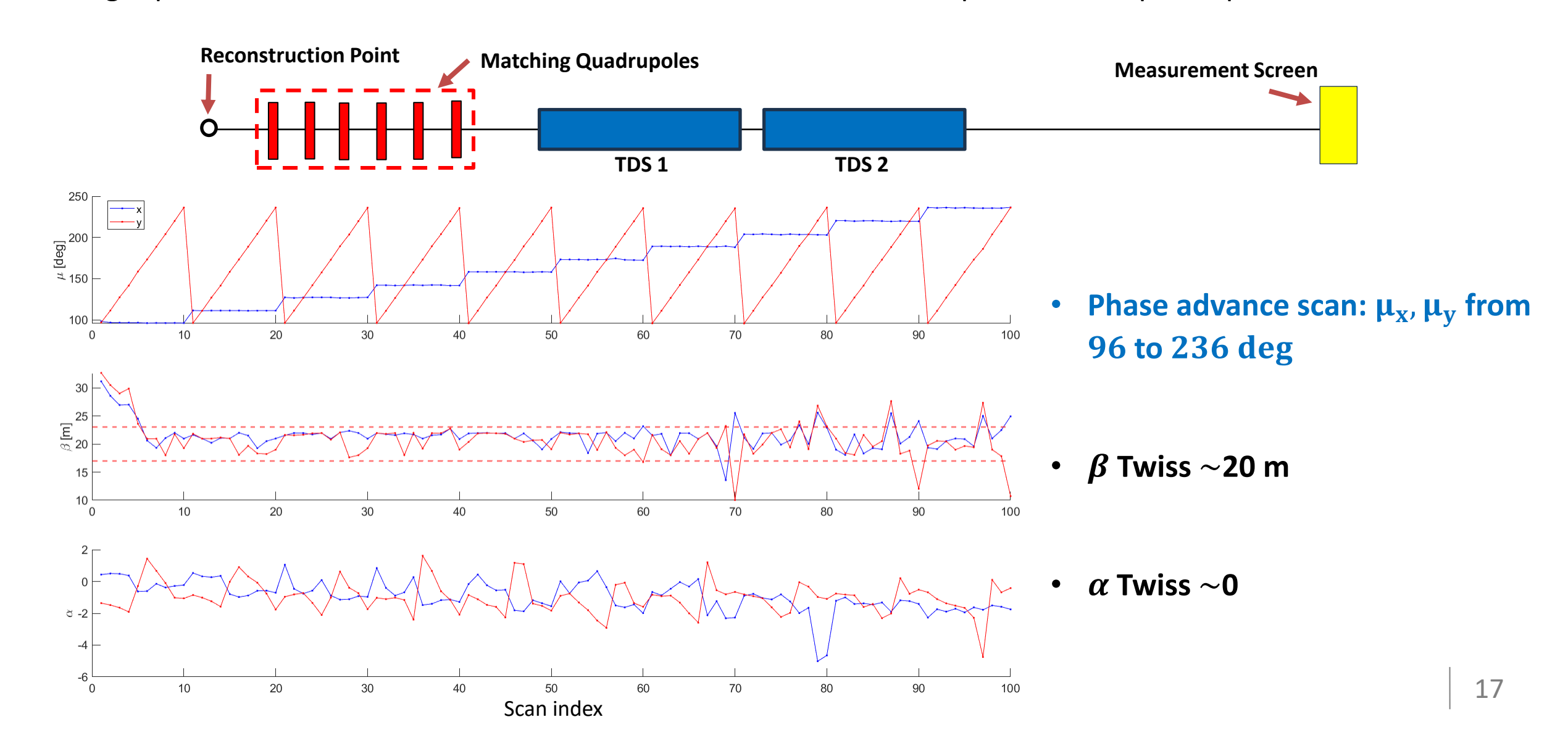
Beam and TDS parameters		
Charge	200 pC	
Energy	3.4 G <i>eV</i>	
TDS length	1.2 <i>m</i>	
Klystron power	28 <i>MW</i>	
TDS Voltage	70 <i>MV</i>	
TDS calibration	$16.5 \mu m/fs$	



5D Reconstruction: Optics simulations



Single-particle simulations have been done to calculate the beam optics for the quadrupole scan

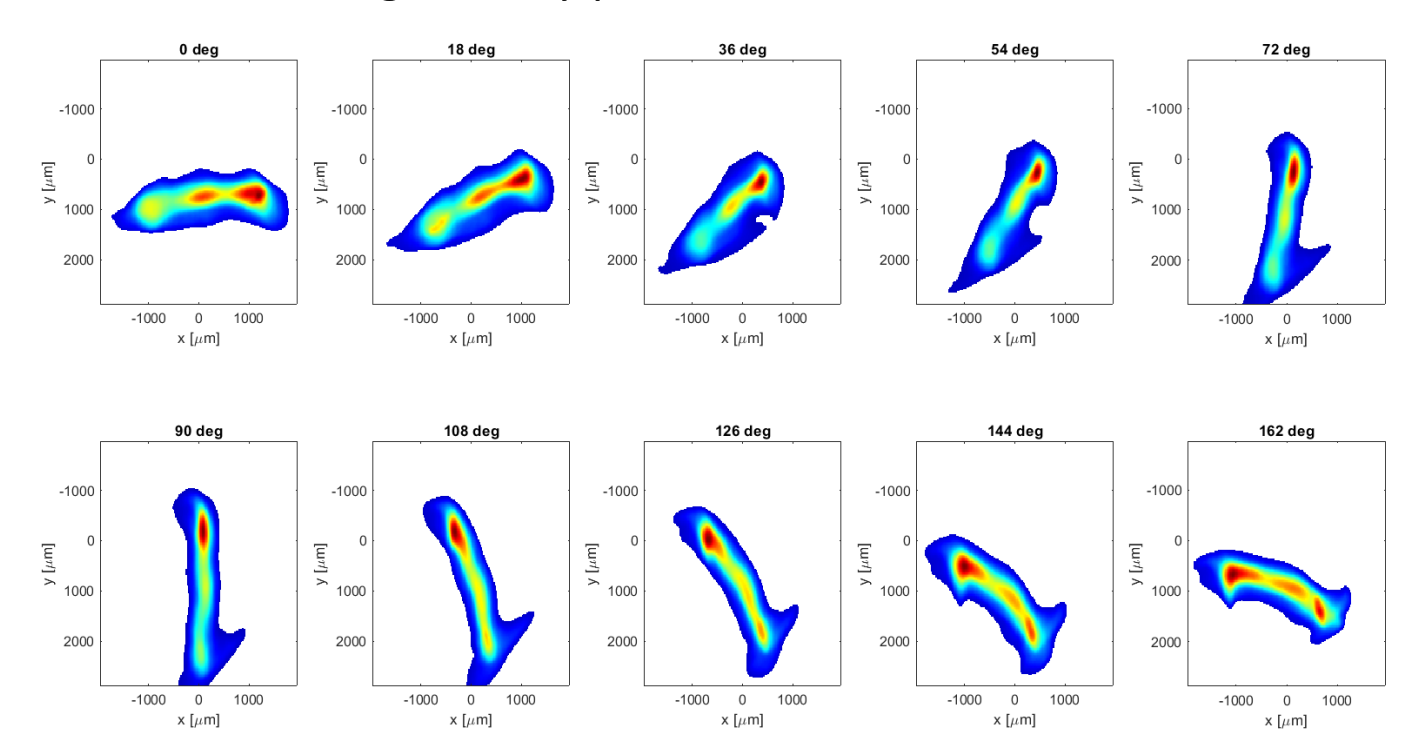




5D Reconstruction: TDS polarizations



- The beam is streaked, covering a polarization range of 180 degrees, and from the centroids, the streaking angle can be evaluated
- The polarization is set by **three phase shifters** that set the single cavity phase and the relative one



Beam Images at different polarizations

$$\theta = \tan^{-1}(\frac{C_y}{C_x})$$

Polarization [deg]	Measured Angle [deg]
0	2.3 ± 0.3
18	19.6 ± 0.3
36	37.9 ± 0.2
54	56.6 ± 0.5
72	74.7 ± 0.5
90	92.9 ± 0.2
108	111.4 ± 0.4
126	130.1 ± 0.2
144	148.2 ± 0.3
162	165.2 ± 0.5

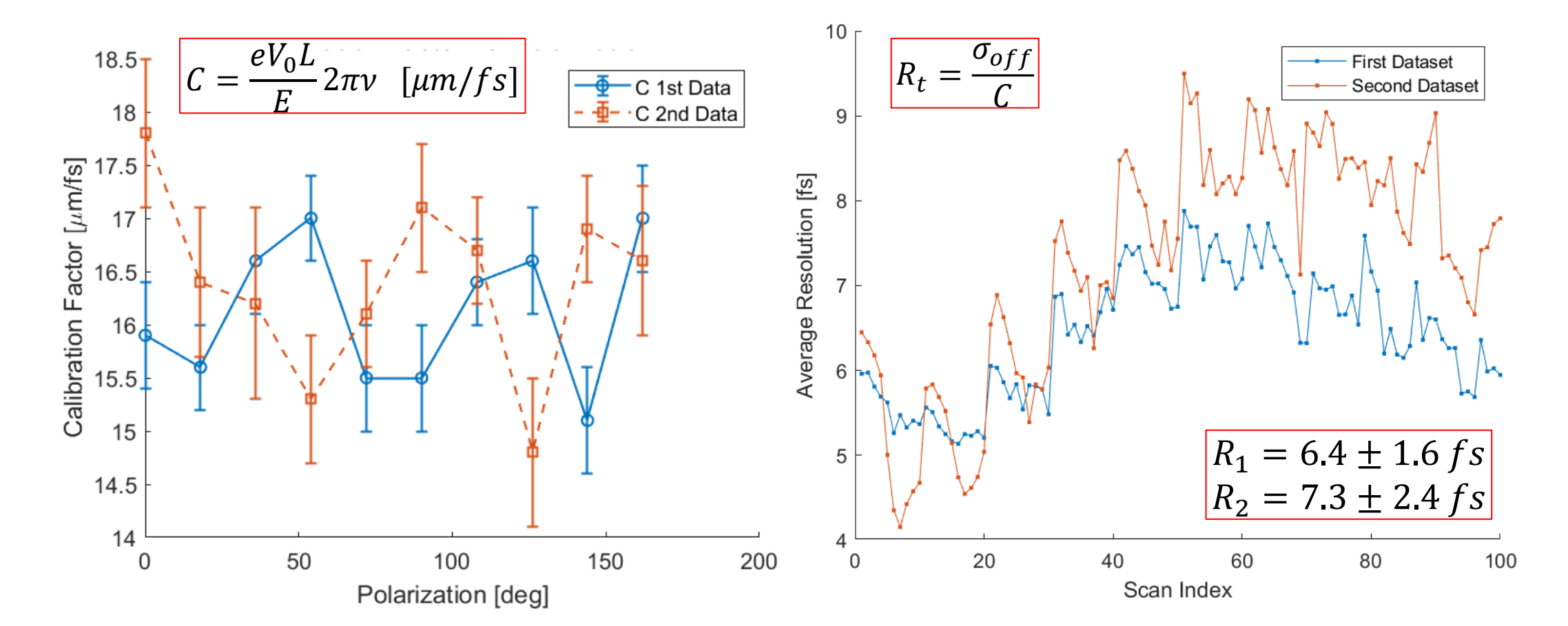
Angle from: Centroid Shift vs RF Phase



5D Reconstruction: Calibration results



- TDS calibration for different streaking angles → Measured the centroid shift when changing the cavity phase
- Expecting a low variation in the calibration factors depending on the streaking angle, due to not using quadrupoles after the TDS





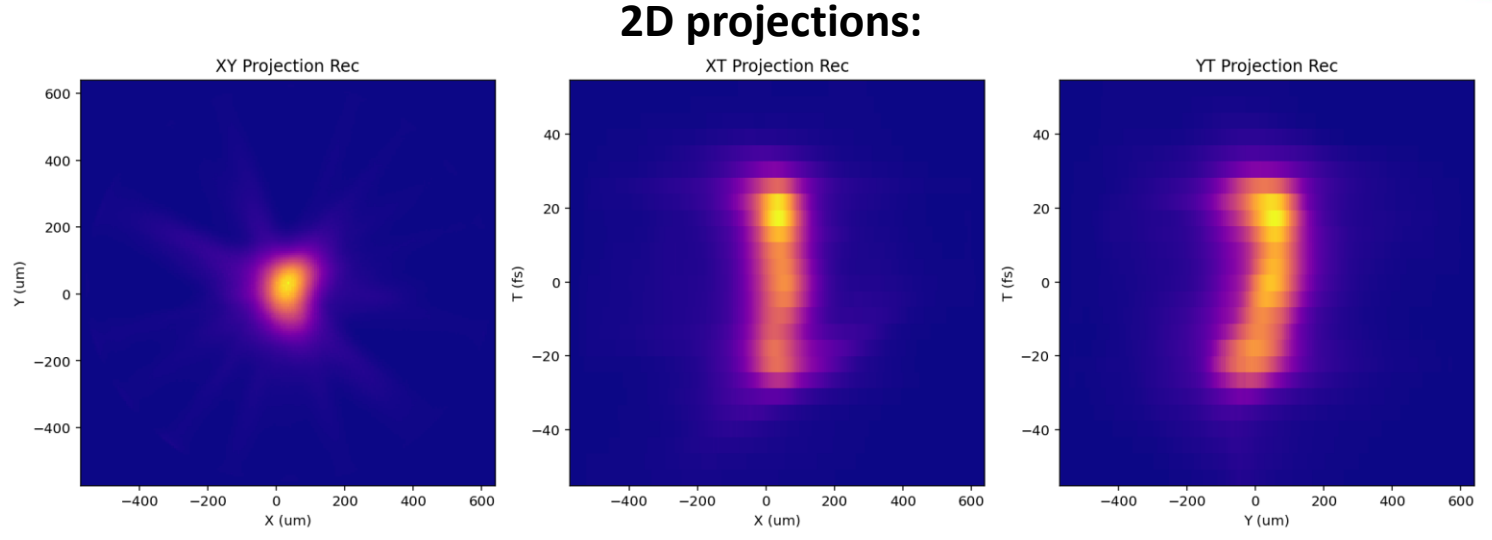
Dataset 1 and 2 – 3D Analysis



- Dataset 1, Optics: $\mu_x = \mu_y = 96 \ deg$
- Slice duration: 4.4 fs (25 slices)

Reconstructed beam parameters:

Quantity	Value
$\sigma_x [\mu \mathrm{m}]$	137 ± 7
$\sigma_y \ [\mu \mathrm{m}]$	135 ± 7
$\sigma_t^{ m rec}$ [fs]	20 ± 4
$\text{FWHM}_t^{\text{rec}}$ [fs]	48 ± 4

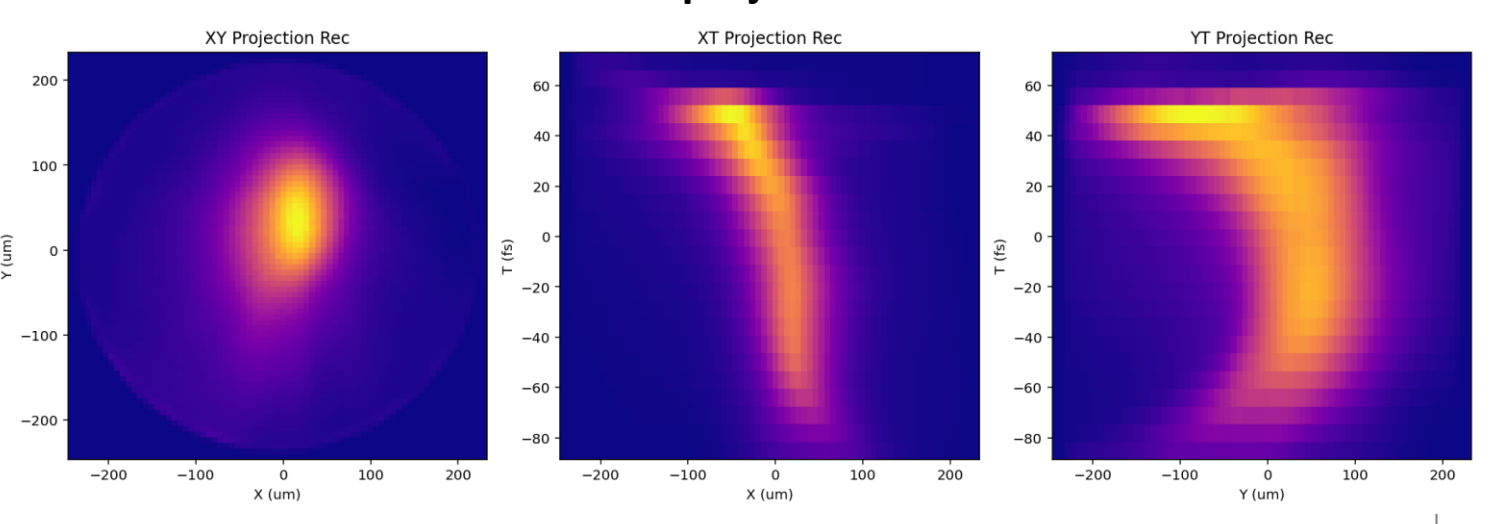


- Dataset 2, Optics: $\mu_x = \mu_y = 96 \ deg$
- Slice duration: 7.1 fs (29 slices)

Reconstructed beam parameters:

Quantity	Value
$\sigma_x [\mu \mathrm{m}]$	70 ± 7
$\sigma_y \ [\mu \mathrm{m}]$	90 ± 7
$\sigma_t^{ m rec}$ [fs]	41 ± 7
$\text{FWHM}_t^{\text{rec}}$ [fs]	97 ± 7

2D projections:

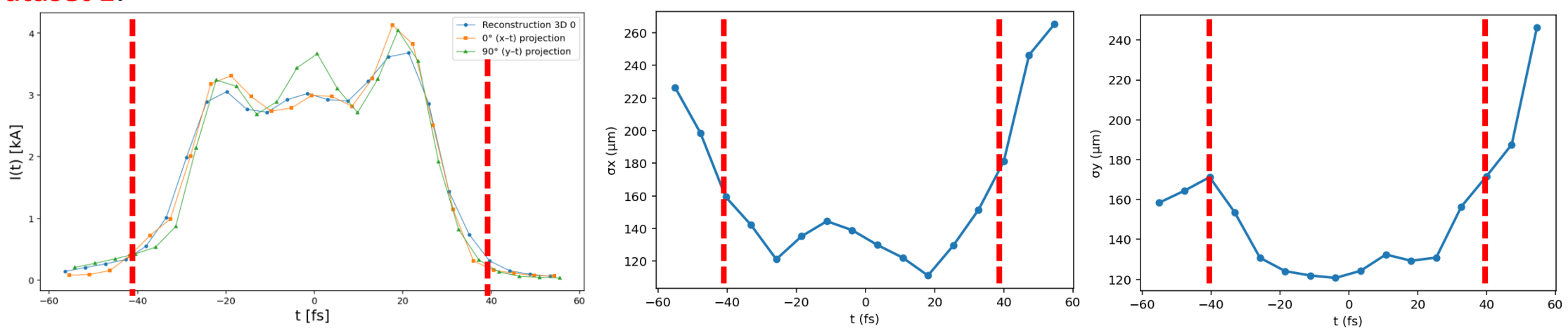




Reconstruced temporal profile

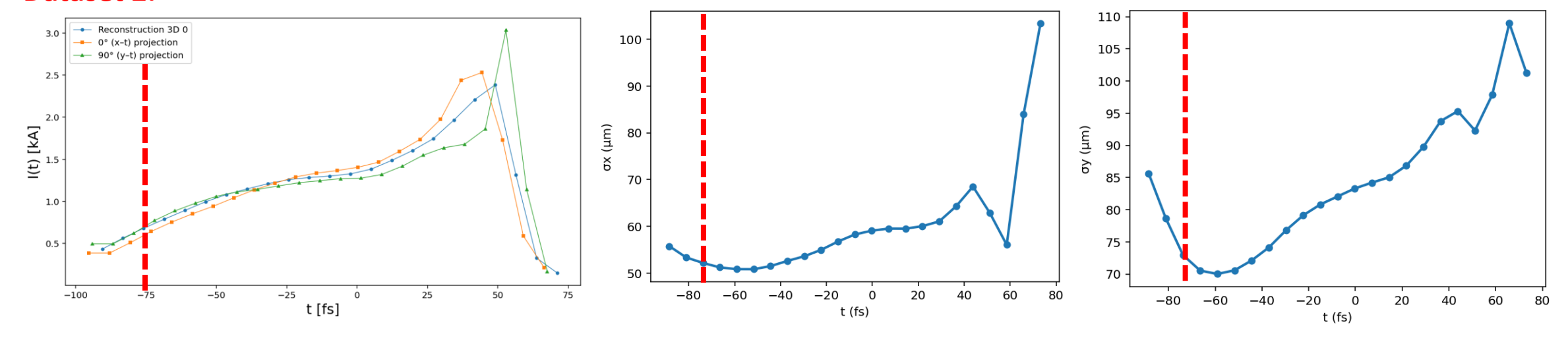


Dataset 1:



> Bunch 1 features a short temporal profile and a regular current distribution

Dataset 2:



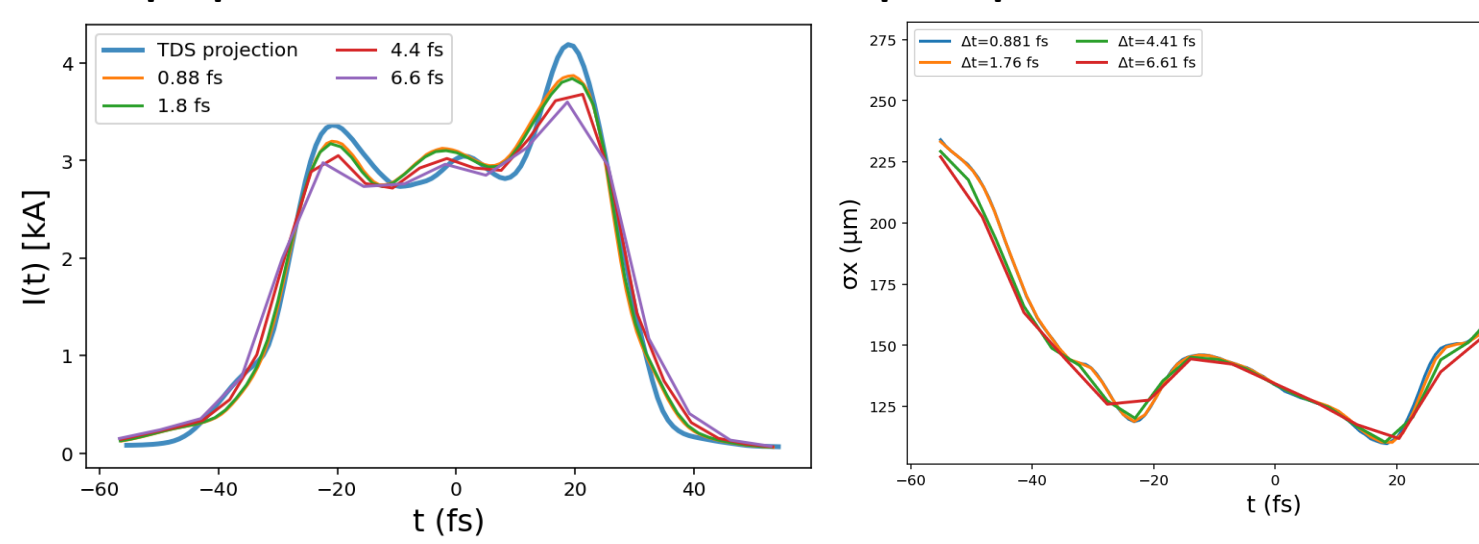
Bunch 2 features a longer temporal profile and a peaked current distribution with a long tail

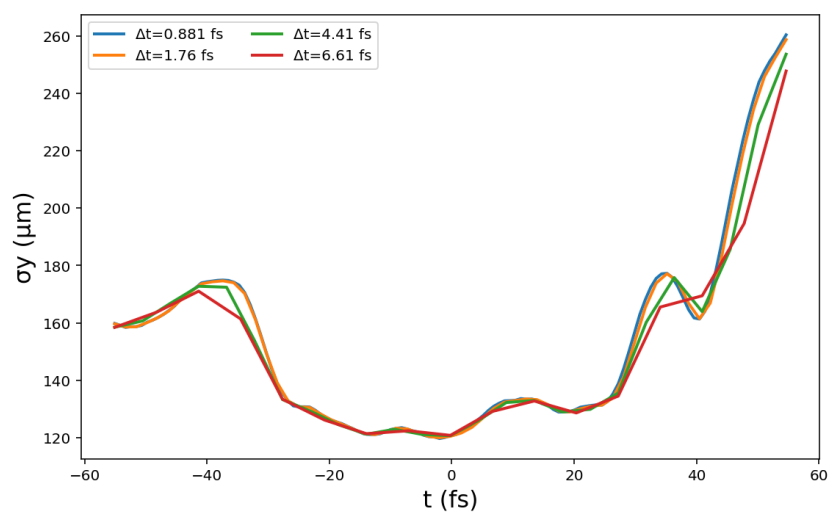


Slice resolution scan analysis



Superposition of the reconstructed temporal profiles and beam sizes for the various slice resolutions:





- As the number of slices increases, the reconstructed value of σ_t progressively converges toward the expected measurement from the conventional TDS measurement
- When the slice resolution Δt_{slice} is shorter than the intrinsic temporal resolution of the TDS measurement, the result is consistent with longer slice resolutions
- In Dataset 2, the scan confirms the trend observed in the first dataset, showing even shorter deviations from the measured bunch duration (obtained from conventional TDS measurement)

Dataset 1:

$N_{ m slice}$	$\Delta t_{\rm slice}$ [fs]	$\sigma_t^{\rm rec}$ [fs]	$\Delta \sigma_t \ [\%]$
125	0.88	19.82	0.56
63	1.76	19.93	1.13
25	4.41	20.38	3.38
17	6.61	20.74	5.13

Dataset 2:

$N_{ m slice}$	$\Delta t_{\rm slice}$ [fs]	$\sigma_t^{\rm rec}$ [fs]	$\Delta \sigma_t \ [\%]$
181	0.90	40.05	0.51
46	3.59	40.55	0.72
28	5.84	40.86	1.45
23	7.19	41.11	2.11

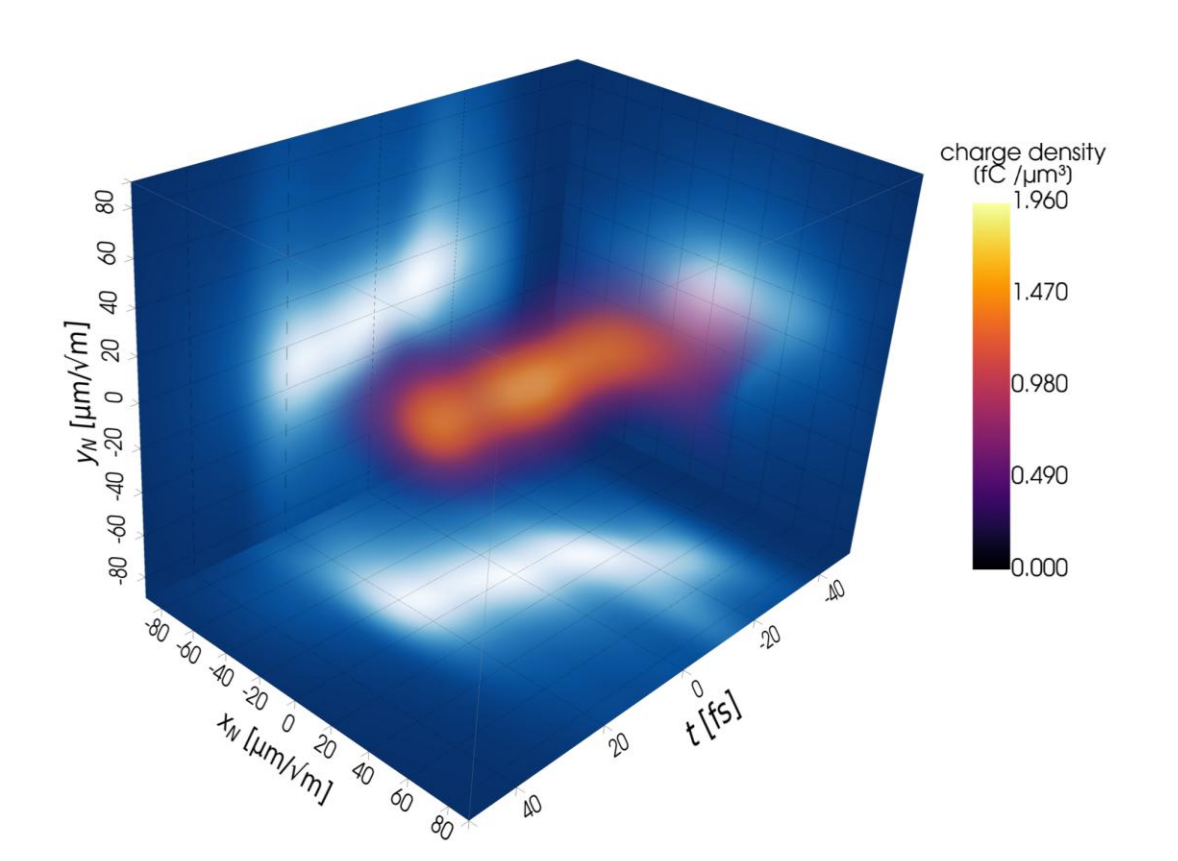


5D Reconstruction: Preliminary results

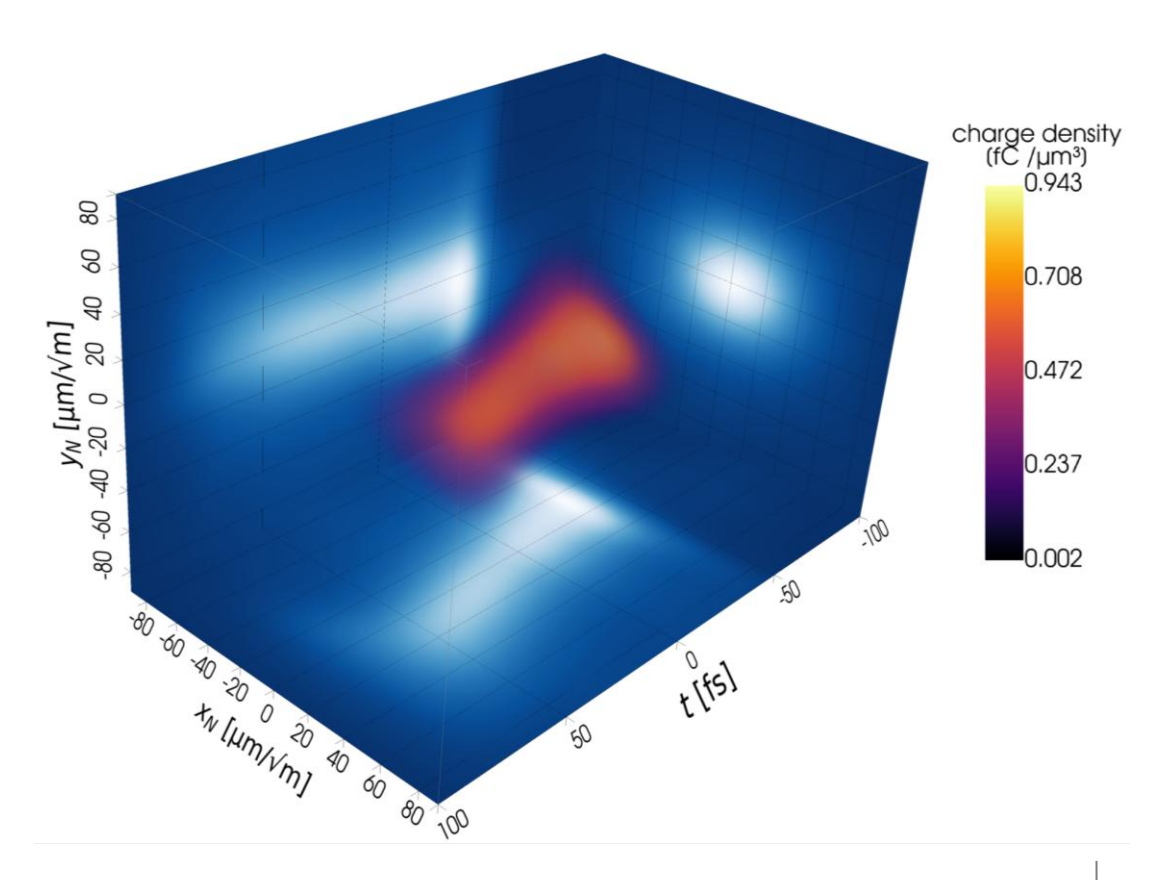


3D beam charge density obtained as a projection of the reconstructed 5D distribution:

Beam 1: High compression $FWHM_t \sim 56 \ fs$



Beam 2: Moderate compression $FWHM \sim 103 \ fs$

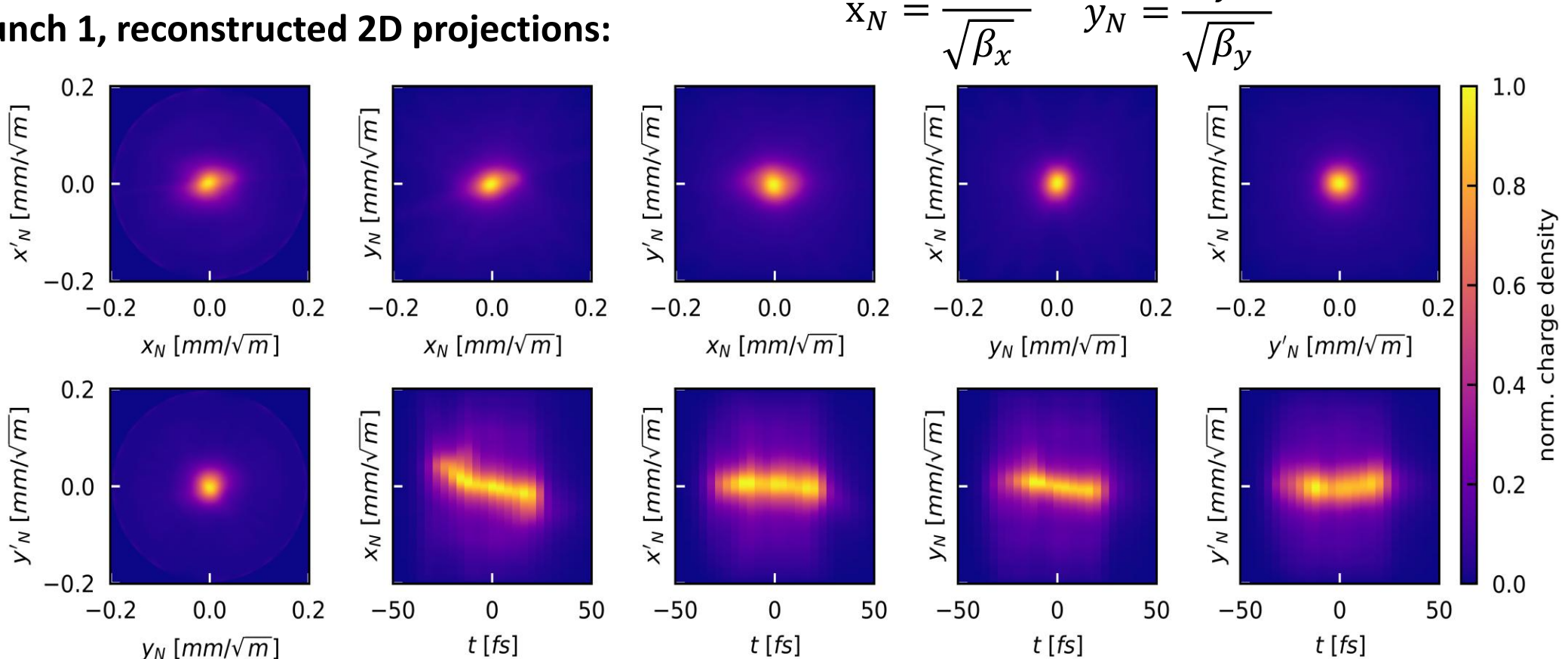




5D Reconstruction: Bunch 1







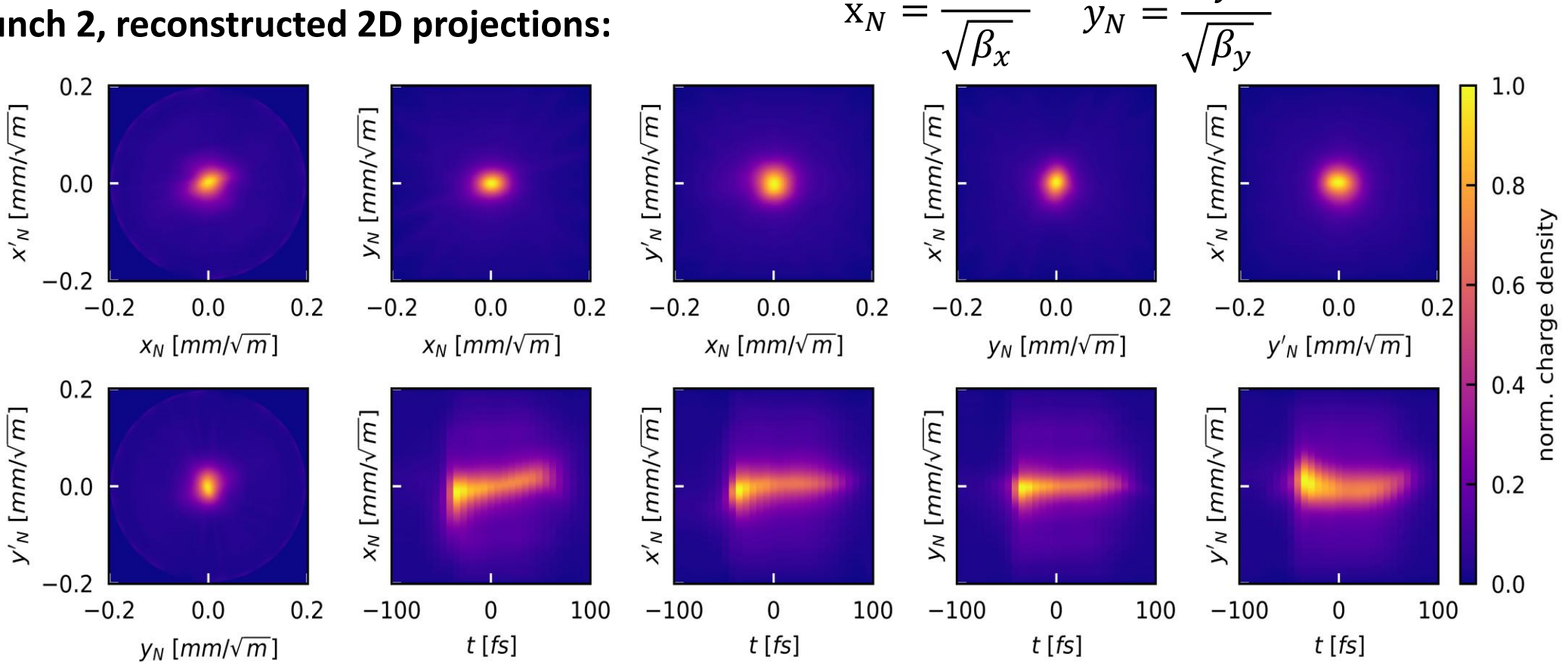
> In the first beam configuration, the high compression produces a very short bunch with an evident tilt in the (x,t) plane



5D Reconstruction: Bunch 2







> In the second beam configuration, the relaxation of the bunch compression reduces the beam tilt



Summary and conclusions



> Summary results

 Determined the resolution limits and performance of the diagnostics beamline at low, middle and high energy, for transverse and longitudinal phase space characterization

Designed and characterized the 50-cell PolariX TDS field maps needed at the low-energy beamline

• Employed the 3D and 5D tomography at the 3 GeV Athos beamline at SwissFEL, to reconstruct beams for two different beam configurations with $\sim fs\ Resolution$





Thank you for your attention



References



- [1] Grudiev, Alexej. Design of compact high power RF components at X-band. No. CERN-ACC-NOTE-2016-0044. 2016.
- [2] Marchetti, Barbara, et al. "Experimental demonstration of novel beam characterization using a polarizable X-band transverse deflection structure." Scientific reports 11.1 (2021): 3560.
- [3] Jaster-Merz, S., et al. "5D tomographic phase-space reconstruction of particle bunches." Physical Review Accelerators and Beams 27.7 (2024): 072801.
- [4] Marx, Daniel, et al. "Reconstruction of the 3D charge distribution of an electron bunch using a novel variable-polarization transverse deflecting structure (TDS)." Journal of Physics: Conference Series. Vol. 874. No. 1. IOP Publishing, 2017.
- [5] Marx, Daniel, et al. "Simulations of 3D charge density measurements for commissioning of the PolariX-TDS." Journal of Physics: Conference Series. Vol. 1067. IOP Publishing, 2018.
- [6] Hock, K. M., and A. Wolski. "Tomographic reconstruction of the full 4D transverse phase space." Nuclear Instruments and Methods in Physics Research Section A: Accelerators, Spectrometers, Detectors and Associated Equipment 726 (2013): 8-16.
- [7] Jaster-Merz, S., et al. "5D tomographic phase-space reconstruction of particle bunches." Physical Review Accelerators and Beams 27.7 (2024): 072801
- [8] Jaster-Merz, S., et al. "Experimental demonstration of a tomographic 5D phase-space reconstruction." arXiv preprint arXiv:2505.13724 (2025).





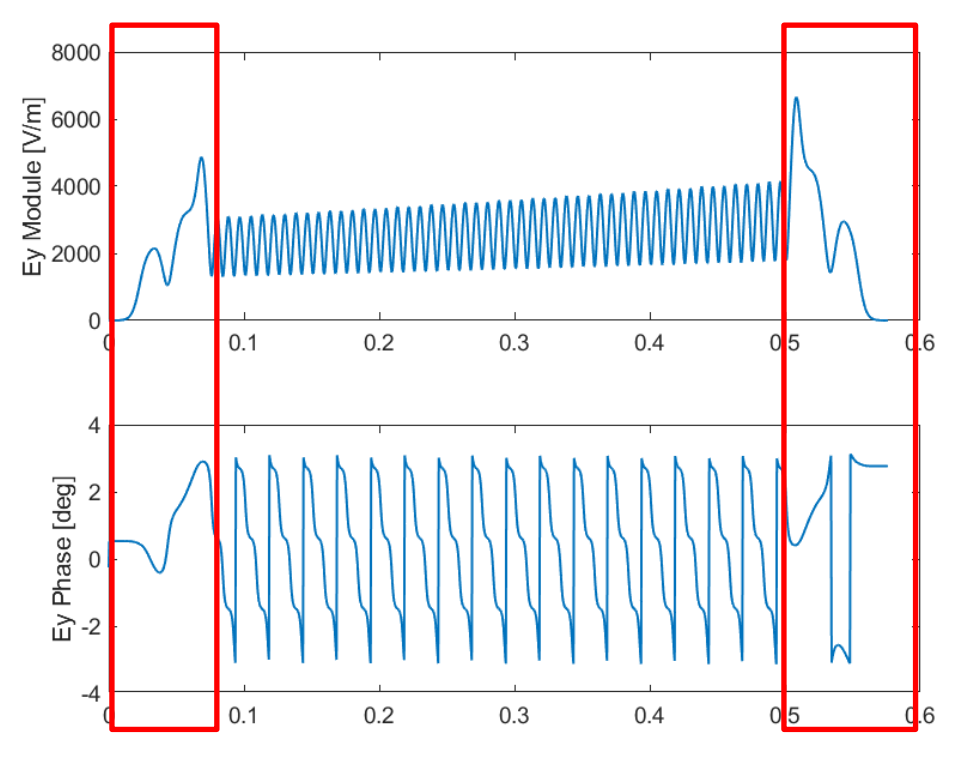
BACKUP SLIDES

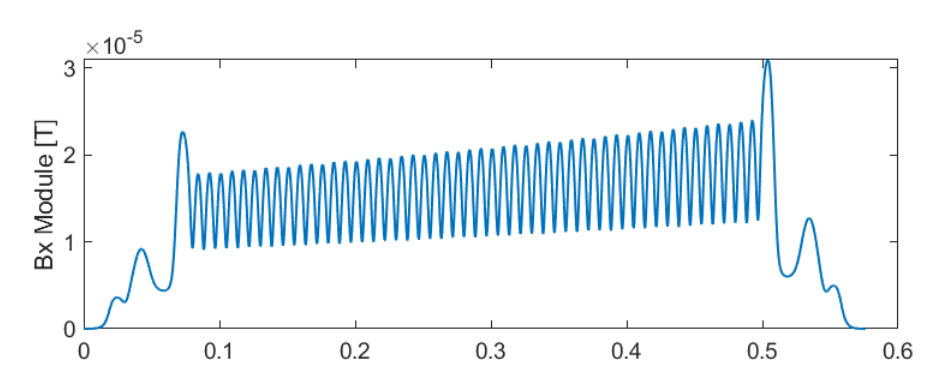


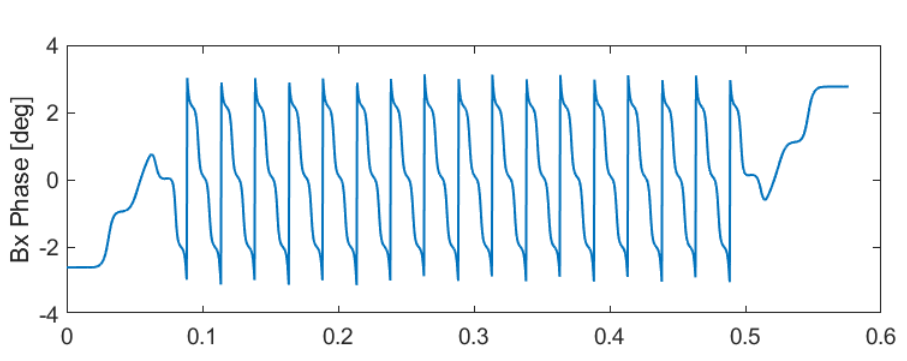
PolariX TDS: Field maps outline



> Fields maps generated with HFSS for the two structures to test the effect on the beam dynamics







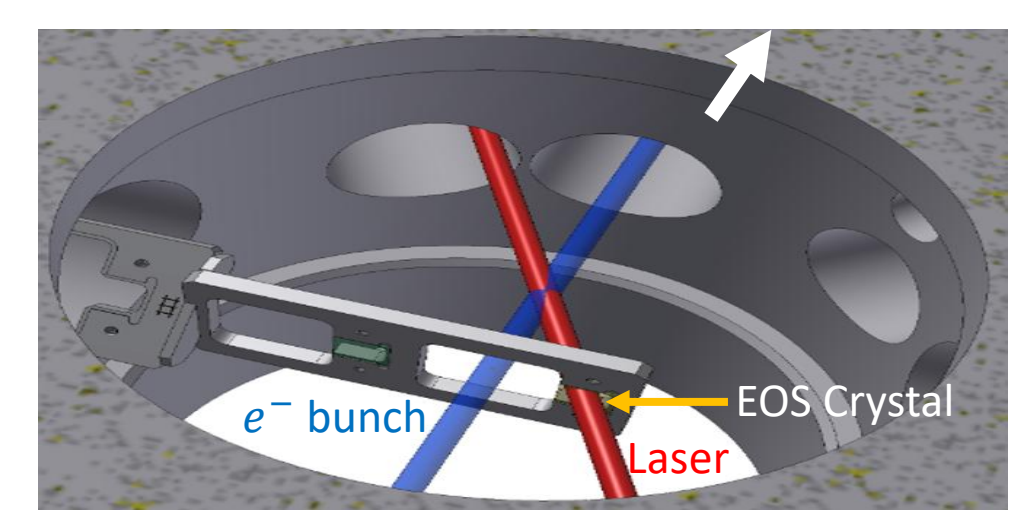
- On-axis field (50-cell)
- 1 W of input power
- Vertical streaking
- Phase Advance per cell: $-\frac{2\pi}{3}$
- Backward travelling wave structure

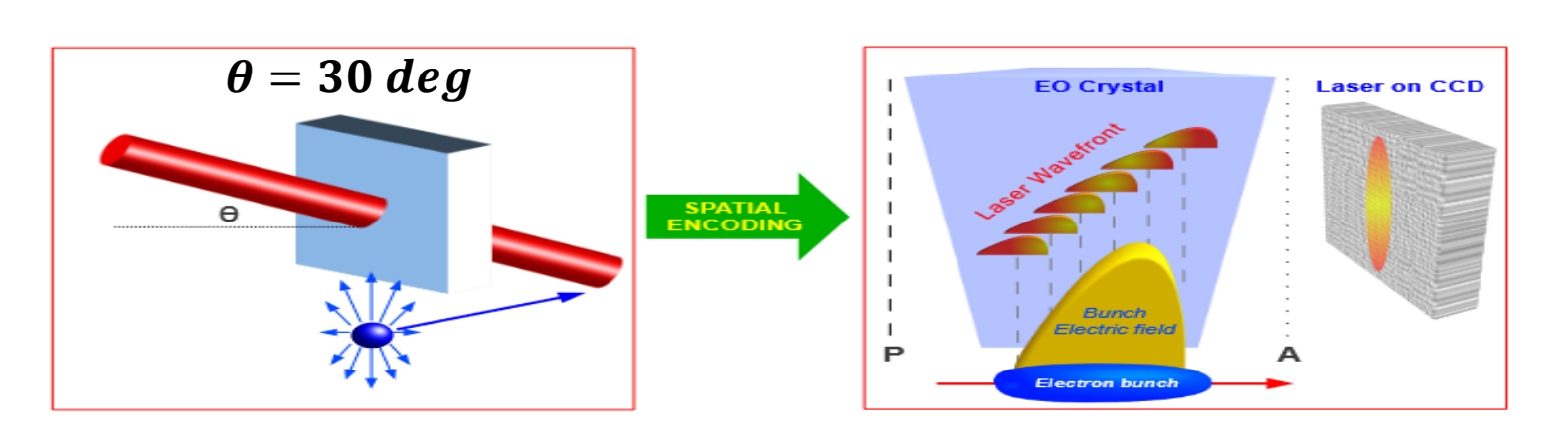


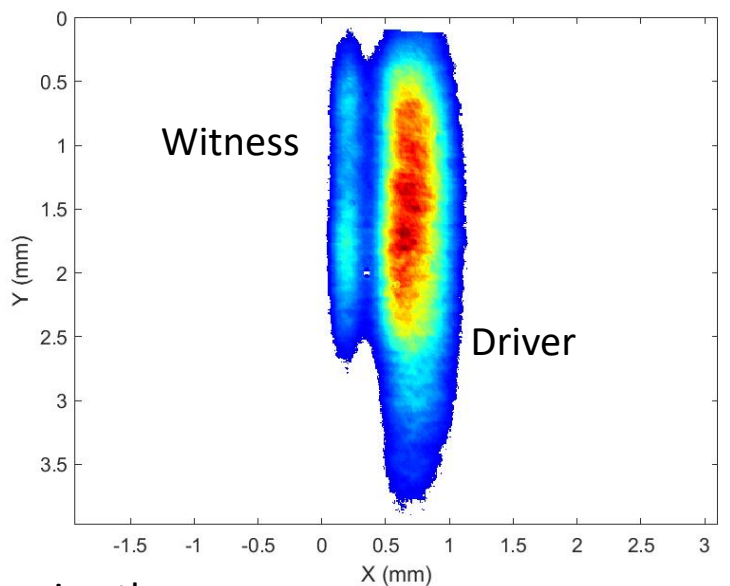
Energy Jitter Measurement at SPARC



- In plasma accelerated beams, the witness energy gain is directly related to the relative distance from the driver beam, so that in the velocity bunch compression scheme, it is affected by the stability of the RF system
- This shot-to-shot jitter requires a complementary single-shot diagnostics to the TDS devices: Electro-Optical Sampling (EOS)
- The witness energy measurement at the high-energy spectrometer is combined with the measurement of the relative distance between the driver and witness beams before the plasma chamber with the EOS





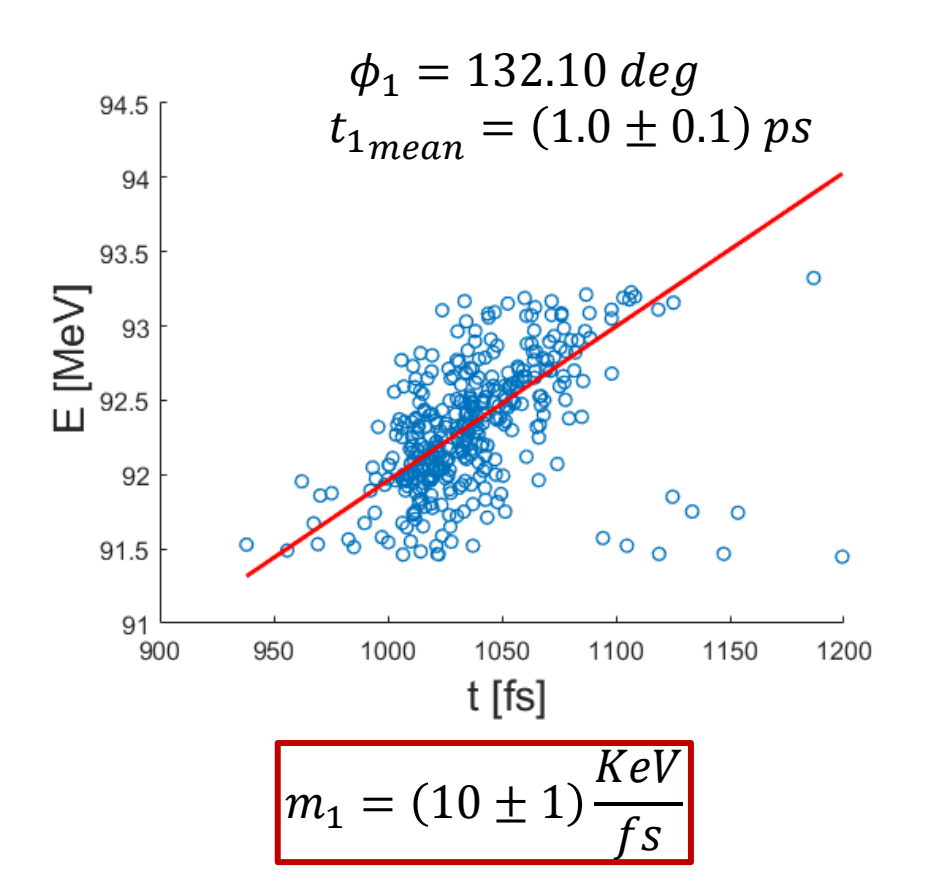


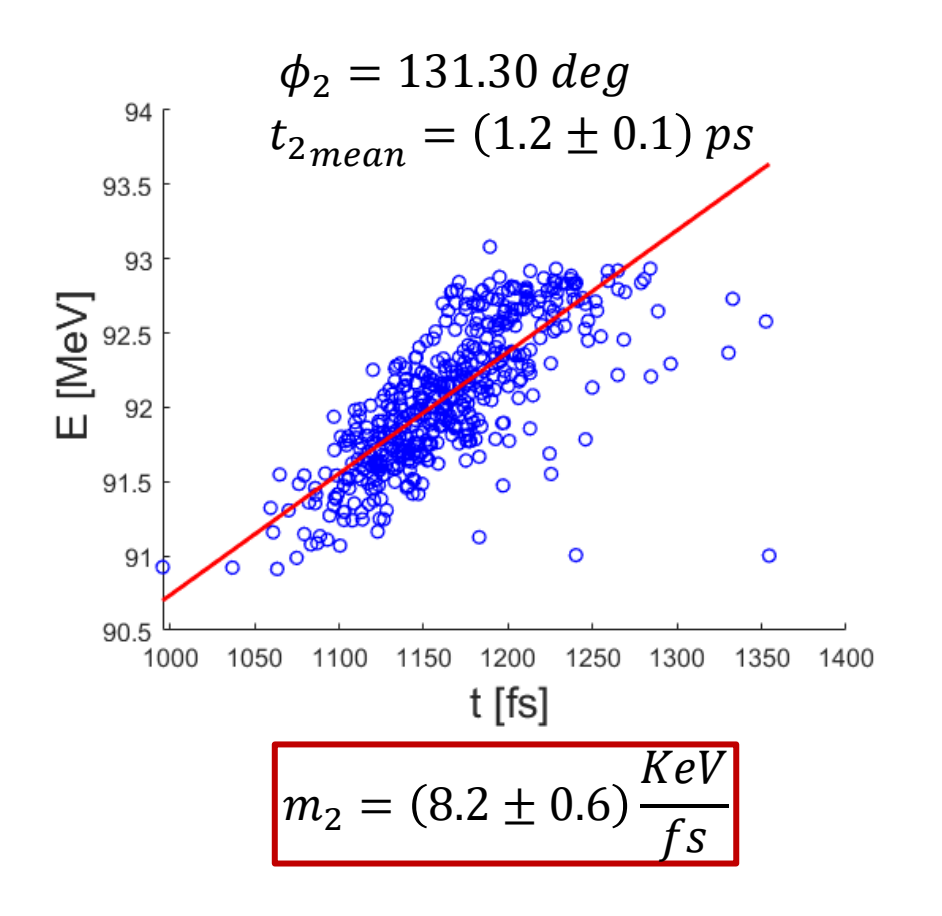
• The resolution in the measurement of the beam arrival time is of fs, so it is suitable for measuring the beam's arrival time and the driver-witness relative distance in the same shot



Measurement Results







- The compression phase is slightly different: when the phase is smaller the compression is larger and therefore, the distance between the bunches increases
- The different slope is dependent on the plasma density (the used density for the experiment is $\sim 10^{15}~cm^{-3}$): the first measurement corresponds to a larger density and so it is higher the slope with respect to the second case



SART tomographic algorithm



> SART (Simultaneous algebraic reconstruction technique) TOMOGRAPHIC ALGORITHM

Working principle:

- 1. Sinogram: set of 1S projections D_i (called ray) in input to the algorithm
- 2. Initial guess $I_0(x, y)$ to calculate the projection $D_{0j} = R_j I_0(x, y)$
- 3. Calculated the projection D_{0j} we define the difference between D_j and D_{0j} and update the initial guess $I_0(x, y)$ to reduce the difference at each iteration

Advantages:

- It is simultaneous because it updates all pixels at the same time
- More accurate and robust than other similar algorithms
- Good reconstruction with few projection angles



Filtered Back Projection algorithm



> FILTERED BACK PROJECTION TOMOGRAPHIC ALGORITHM

Working principle:

- 1. 2D Projection of 4D distribution $I(x,y) = \int \int f_B(x,x',y,y') dx' dy'$
- 2. $(x, x') \Rightarrow (x_1, x_1')$ after a rotation $\theta_x \Rightarrow I(x_1, y) = P_{y, \theta_x}(x_1)$: Projection
- 3. Consider y as constant, and work only on the x,x' variables
- 4. Apply Fourier transform to P: $S_{y,\theta_x}(w) = \int_{-\infty}^{\infty} P_{y,\theta_x}(x_1) e^{-2\pi i w x_1} dx_1$
- 5. Apply high-pass filter and revert the transform: $Q_{y,\theta_x}(x_1) = \int_{-\infty}^{\infty} S_{y,\theta_x}(w) |w| e^{2\pi i w x_1} dw$
- 6. Compute the back-projection: $g_{y}\left(x,x'\right)=\int_{-\pi}^{\pi}Q_{y,\theta_{x}}\left(x_{1}\right)d\theta_{x}$
- 7. Repeating the same process for y gives the 4D distribution



Athos beamline optics



- The optics has been calculated to match the Twiss parameters to screen
- Since there are no quadrupoles active, but only a drift after the TDS, the beta function at the TDS center and the beam size at the screen are dependent parameters

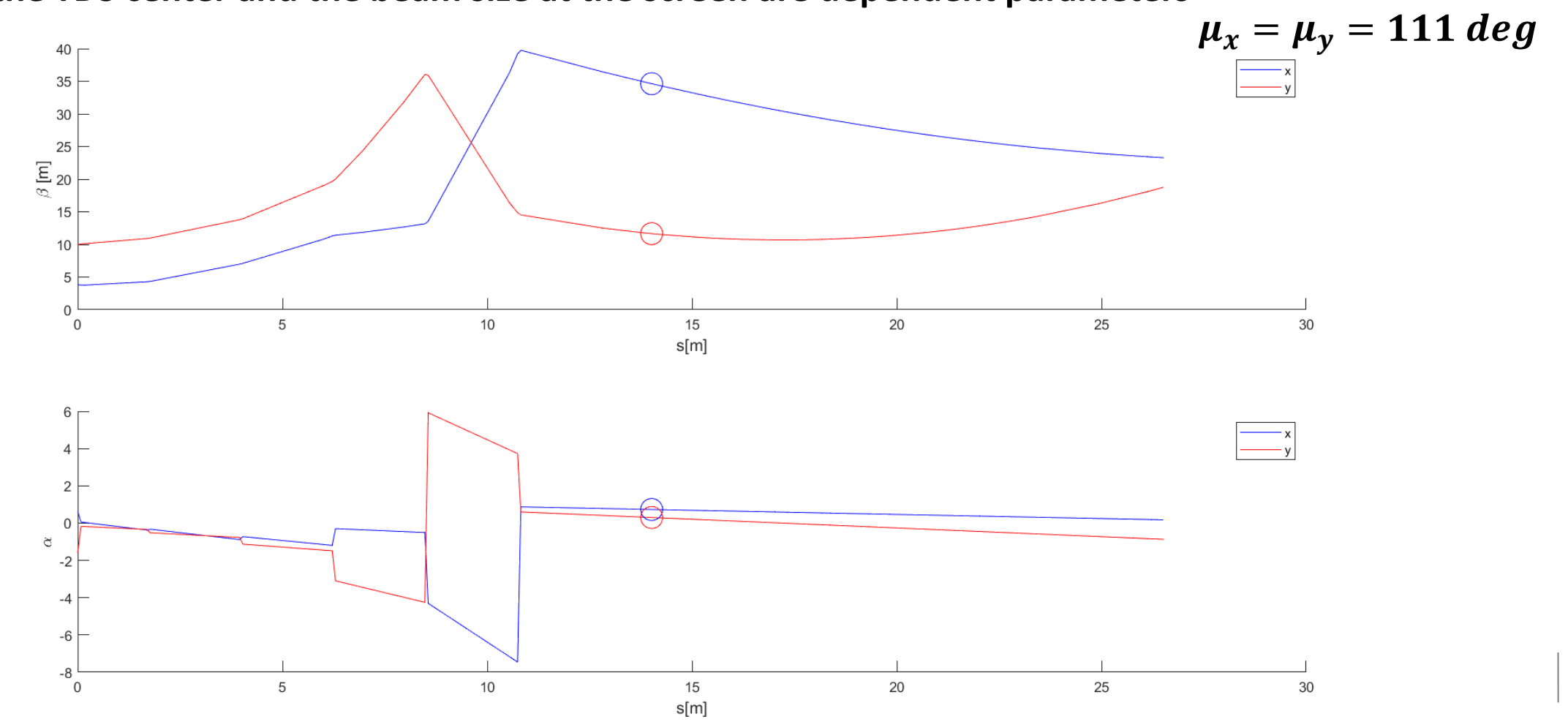




Image treating methodology



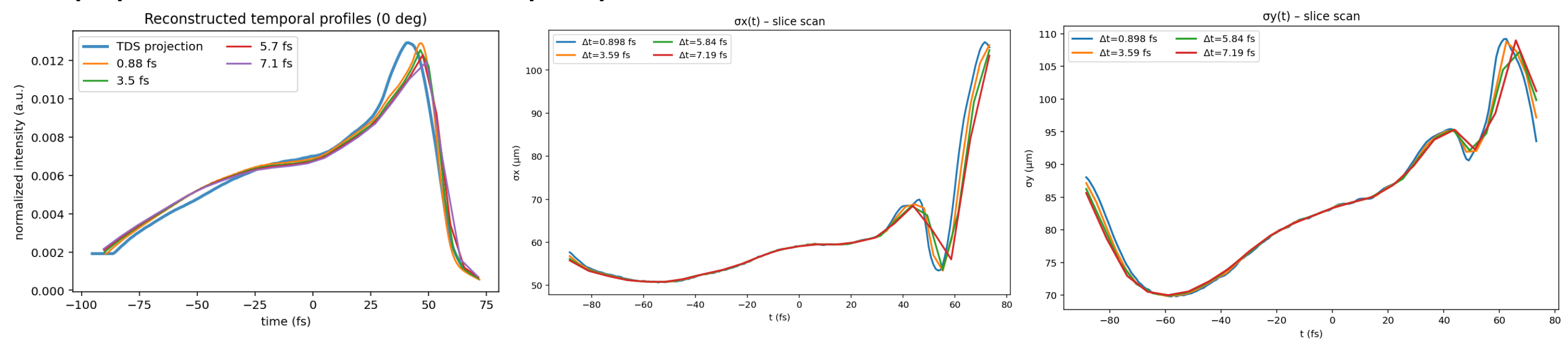
- > The images have to be prepared to perform the tomographic reconstruction:
 - 1. Remove background and apply gaussian filters to the images
 - 2. Rescale images to have square pixels
 - 3. Rotate the images by the streaking angle
 - 4. Apply the calibration factor to the streaking axis and rescale the images to have the same temporal scale
 - 5. Center the images
 - 6. Set the ROI to select only the beam
- > This allows for the reconstruction, minimizing the artifacts that can arise from the disalignment in the images and from background contributions



Dataset 2 – Slice scan analysis



• Superposition of the reconstructed temporal profiles and beam sizes for the various slice dimensions:



 In Dataset 2, the slice duration scan confirms the trend observed in the first dataset, showing even shorter deviations from the measured bunch duration (obtained from conventional TDS measurement)

$N_{ m slice}$	$\Delta t_{\rm slice}$ [fs]	$\sigma_t^{ m rec}$ [fs]	$\Delta \sigma_t \ [\%]$
181	0.90	40.05	0.51
46	3.59	40.55	0.72
28	5.84	40.86	1.45
23	7.19	41.11	2.11